Winter 12-22-1959

A Theoretical and Experimental Analysis of a Hall Generator

David L. Endsley

A THEORETICAL AND EXPERIMENTAL ANALYSIS OF A HALL GENERATOR

by
David L. Endsley

A Thesis

Submitted in Partial Fulfillment of

the Requirements for the Degree of

Master of Science in Electrical Engineering

The University of New Mexico

This thesis, directed and approved by the candidate's committee, has been accepted by the Graduate Committee of the University of New Mexico in partial fulfillment of the requirements for the degree of

MASTER OF SCIENCE

E. H. Castetter

DEAN

December 22, 1959

DATE

Thesis committee

W. W. Grannemann

CHAIRMAN

A. W. Mellon

E. L. Jordan

ACKNOWLEDGMENTS

The writer wishes to express his appreciation to Dr. W. W. Grannemann for his guidance. He wishes also to thank Wallace L. Anderson and Bill J. Harper for their helpful suggestions, and Jack Bresenham for his efforts in obtaining the experimental data.

TABLE OF CONTENTS

LIST OF FIGURES

Figure

CHAPTER I

INTRODUCTION

Since the advent of the transistor in 1948, numerous semiconductor materials have been produced in the continuing search for more reliable and efficient transistors. One group of these materials possesses extremely high mobility and is useful in new devices which do not utilize transistor action. These devices make use of the "Hall Effect", a phenomenon discovered in 1879. The "Hall Effect" occurs when a perpendicular magnetic field is applied to a conductor carrying current. Under these conditions it is found that in addition to the longitudinal electric field normally present a transverse field is produced so that the current and the electric field are no longer parallel.

There are several "Hall Effect" devices commercially available at the present time for use in circuit applications. Westinghouse Electric Company produces the 803 Hall generator for instrument and analog computer applications, and Ohio Semiconductors Inc. produces the HS-51 Halltron and the HR-31 Halltron for numerous other uses.

1.1 Purpose of the Study. This is a study of the behavior of a "Hall Effect" device by theoretical and experimental

methods to determine if its operation may be predicted for various magnetic fields, output resistances, operating temperatures, input resistances, input control currents, and device construction.

This information should prove useful in the design of a circuit where the use of a "Hall Effect" device is contemplated.

1.2 Scope of the Study. All of the experimental work was performed on the HS-51 Halltron manufactured by Ohio Semiconductors, Inc., Columbus, Ohio. The Halltron appeared on the market in the early part of August 1958, and since that time Westinghouse Electric Co. has produced an equivalent device called the "Hall Generator". Since the experimental work performed in this study was nearing completion by the time the Westinghouse device was available, no comparison was made between the two units.

The theoretical work was first carried out for the general case using a semiconductor slab, after which the results were compared to the experimental results obtained from the HS-51 Halltron.

CHAPTER II

BACKGROUND

2.1 Hall Effect. Recent emphasis on semi-conductor research has rediscovered the Hall Effect[1] as a measurement tool more sensitive than the best chemical analysis available. In semiconductor research it has proven invaluable in determining accurate figures on carrier concentrations, mobilities, density of foreign atoms and carrier types. As mentioned previously, when a conductor carrying a current is subjected to a magnetic field perpendicular to the direction of the current flow, the Hall effect occurs; that is, a voltage is developed along the perpendicular dimension of the conductor and is proportional to the product of current density and magnetic field. The relationship of input currents, Hall voltages, and magnetic field is illustrated in Figure 1.

The potential gradient in the y direction is a function of the current density, applied magnetic field, and a proportionality constant called the "Hall Constant". Mathematically this can be expressed as:

$$\text{Grad } V_H = -RiH$$

---

[1] O. Lindberg, "Hall Effect", Proc. of the IRE, Vol. 40, pp. 1414-1419, Nov., 1952

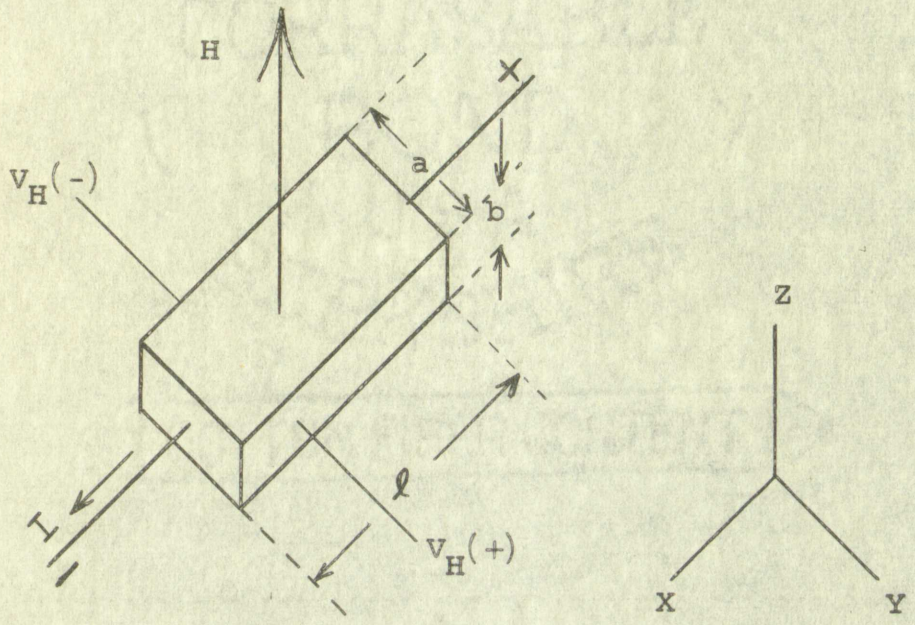

VOLTAGE COMPONENTS FOR CONDUCTION BY ELECTRONS IN A MAGNETIC FIELD

FIG. 1

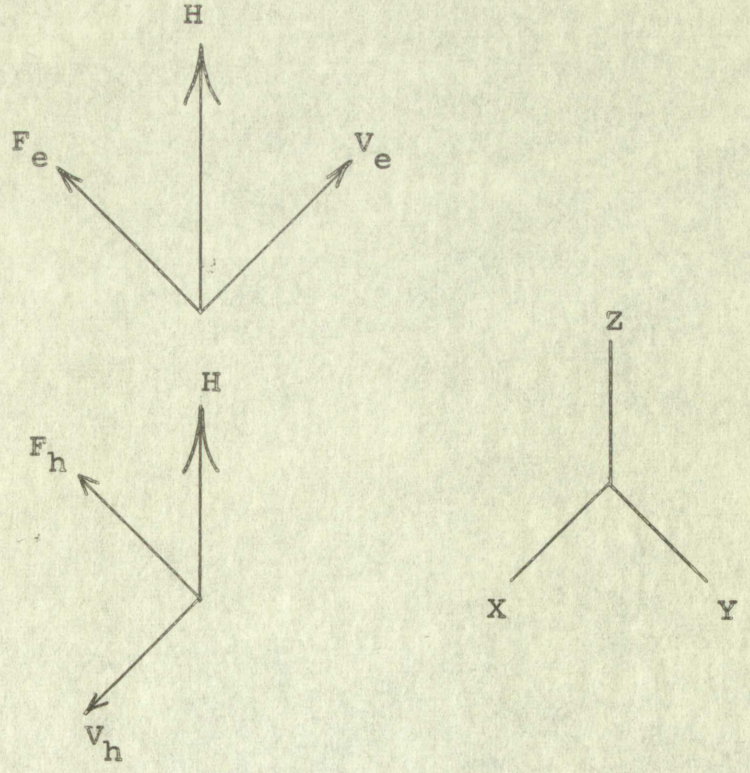

FORCE ON HOLES AND ELECTRONS BY A MAGNETIC FIELD

FIG. 2

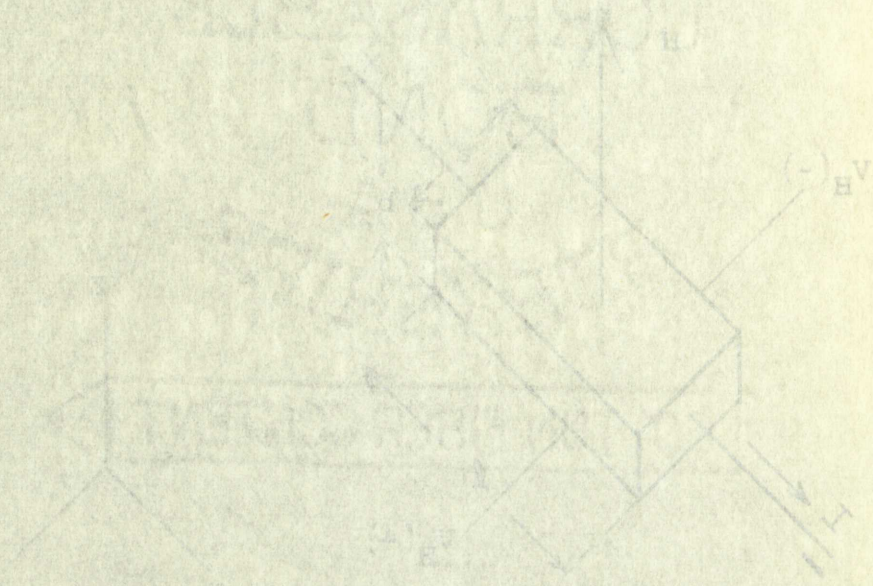
(-)
I

Grad $V_H = -E_H$, where E_H is the Hall electric field, i is the current density, H is the applied magnetic field, R is the Hall constant, and I is the total current.

Assuming the dimension of the slab to be of width a, and thickness b, the Gradient $V_H = -RiH$ can be rewritten as the Gradient $V_H = \frac{-RIH}{ab}$, or $V_H = \frac{-RIH}{b}$.

The Hall phenomenon can be explained by considering the nature of particles in conduction. With the application of an electric field the charged particles drift longitudinally as indicated in Fig. 1. Under the influence of a magnetic field the current carriers experience a force $\frac{e}{c}(v_x \times H_z)$ which then deflects to the edges of the sample. In the semiconductor case both holes and electrons are the current carriers and the effect of the magnetic field is to deflect them to the same side of the sample. The cross product $v_x \times H_z$, where v_x is the velocity of the carriers in the minus x direction and H_z the magnetic field in the z direction, produces a force that deflects an electron in the negative y direction.

Since the hole has a plus charge and its velocity is in the positive x direction the cross product yields a force which deflects it in the negative y direction also. The vector relationships are illustrated in Fig. 2.

The charge created by the deflected carriers will continue to build up on the edges until the force created by the non-uniform charge distribution equals the deflection force

caused by the magnetic field. The magnetic deflection force can be equated to the force created by the concentration of current carriers on the edges by the mathematical expression $e\vec{E} = \frac{e}{c}(\vec{v} \times \vec{H})$ where $\vec{v} = \vec{i}v_x$, $\vec{H} = \vec{k}H_z$, then $e\vec{E} = \frac{e}{c}(\vec{i}v_x \times \vec{k}H_z)$. The current density in x direction can be expressed as $i = nev$ where n is the carrier concentration, then $v = \frac{i}{ne}$ and $eE = \frac{iH}{nec}$, i and H can be replaced by i_x and H_z since $i_y = 0$, $i_z = H_y = 0$. The previous expression can be equated to RiH to obtain an expression for the Hall constant $R = \frac{1}{nec}$.

The Hall constant derived is valid only for metals and impure semiconductors since the truth of the particle type conduction was assumed. A more valid Hall constant can be obtained by considering Boltzman's distribution of carrier velocity. The formula generally used for the Hall constant is $\frac{3\pi}{8}(\pm\frac{1}{nec})$ where the negative sign is used for an n-type material and plus for p-type.

When both electrons and holes are present, the Hall constant becomes much more involved. W. Shockley[2] arrives at an expression which is a complicated average of the Hall constant and conductivity for each type of carrier involved. The Hall constant derived for holes and electrons is $R_h = \frac{-nb^2+p}{(nb+p)^2ec}$, where b is the ratio of electron to hole mobility, n is the

[2] W. Shockley, Electrons and Holes in Semiconductors, D. Van Nostrand Company, New York, N. Y., 1950, p. 216

density of electrons, p the density of holes, e the charge on the electron, and c the speed of light.

2.2 Thermomagnetic and Galvanomagnetic Phenomena in Semiconductors. When the Hall type measurement is used to determine properties of certain semiconductors, several associated effects must be accounted for. The magnitudes of these effects are of a sufficient degree to give an erroneous value for the Hall voltage, thus indicating erroneous properties for the semiconductor in question. Since these effects contribute to the limitations of the theoretical and experimental comparison presented in this study, a brief description of the phenomena will be given. Other than the Hall effect there are three thermomagnetic and galvanomagnetic effects[3,4] which contribute to the measured voltage. They are the Ettingshausen effect, the Nernst effect, and the Righi-Leduc effect.

In the Ettingshausen effect, a permanently maintained temperature gradient will appear if an electric current is subjected to a magnetic field perpendicular to the direction of its flow. This temperature gradient is proportional to the product of the current density and magnetic field.

---

[3] L. L. Campbell, Galvanomagnetic and Thermomagnetic Effects, Longmans, Green and Co., New York, N.Y., 1923

[4] A. Sommerfeld and N. H. Frank, "The Statistical Theory of Thermoelectric, Galvanomagnetic, and Thermomagnetic Phenomena in Metals", Review of Modern Physics, Vol. 3, p. 1, 1931

$$\frac{\Delta T}{a} = PiH \qquad i = \frac{I}{ab}$$

$$\Delta T = \frac{PIH}{b}$$

ΔT is the difference in temperature between the edges of the sample, i is the current density, I the total current, H the magnetic field perpendicular to the direction of current flow, P the Ettingshausen coefficient, a the width of the sample, and b the thickness of the sample.

The Nernst and Righi-Leduc effects are similar to the Hall Effect except that they are produced by a thermal current and perpendicular magnetic field rather than by an electric current and a perpendicular magnetic field.

In the Nernst Effect, a potential appears in the y direction if a thermal current flows in the x direction and a magnetic field in the z direction.

$$E_n = Q \frac{WH}{K}$$

E_n is the transverse Nernst potential gradient, w the thermal current density, K the thermal conductivity of the sample, and Q the Nernst coefficient.

In the Righi-Leduc effect, a temperature gradient is produced in the y direction when a thermal current flows in the x direction, and a magnetic field in the z direction.

$$\frac{\Delta T}{a} = S \frac{WH}{K}$$

ΔT is the difference in the temperature between the edges of the sample, S the Righi-Leduc coefficient and a, w, H, K are as previously mentioned.

The generation of heat by the conventional IR drop plus the thermal energy contributed by the thermomagnetic and galvanomagnetic phenomena produce variations in the conductivity of the semiconductor material which complicate the theoretical and experimental comparison.

2.3 Indium Antimonide. Among the elements in the periodic table there are many possible combinations. Of the various combinations investigated for their semiconducting properties, a few have shown promise, such as the fourth group elements of the II-V I and I-VII compounds and the III-V compounds, whose semiconducting properties have been known only since 1952.

2.31 Basic Properties. One of the most prominent of these III-V compounds is Indium Antimonide (InSb) which is similar to gray tin in that it has the same lattice structure and lattice constant. Of all the III-V compounds, InSb has probably the most profound properties. It has the lowest melting point, namely 523° C and contrary to gray tin, it exists in only one modification. The mobility of InSb is approximately $70000 \frac{cm^2}{volt\ sec}$ highest of the III-V compounds, but recently mobilities of $500000 \frac{cm^2}{volt\ sec}$ have been obtained. InSb is

ΔT is the difference in the temperature between the ends
of the sample, S the Seebeck coefficient and σ, β, γ,
K are as previously mentioned.

The generation of heat by the converse Ettingshausen
the thermal energy conducted by the thermomagnetic and
galvanomagnetic phenomena produce cooling in the conductivity
of the semiconductor material which complicates the experimental
and experimental comparison.

2.3 Indium Antimonide. Among the elements in the
periodic table there are many possible combinations of the
various combinations investigated for their semiconductivity
properties, a few have shown promise, such as the fourth group
elements of the II-V I and I-VII compounds and the III-V compounds, whose semiconducting properties have been known only
since 1952.

2.31 Basic properties. One of the most prominent of these
III-V compounds is Indium Antimonide (InSb) which is unique in
many ways in that it has the same lattice structure and lattice
constant. Of all the III-V compounds, InSb has probably the
most profound properties. It has the lowest melting point,
namely 523° C and contrary to many others, it exists in only one
modification. The mobility of InSb is approximately
7000 $\frac{cm^2}{volt\ sec}$ highest of the III-V compounds, but recently
mobilities of 50000 $\frac{cm^2}{volt\ sec}$ have been obtained in

quite temperature sensitive, more so than the other III-V compounds. The energy band gap for InSb is approximately .18 electron volts, which means that intrinsic conduction contributes to the total conductivity at lower temperatures than most compounds. At room temperature the conductivity is about 200 ohm^{-1} cm^{-1}. Indium antimonide is metallic in appearance, similar to germanium, and is quite brittle.

2.32 Temperature and Magnetic Field Effect on Conductivity. H. Welker and co-workers[5] conducted conductivity and Hall effect measurements on six samples of InSb for various temperatures. Four of the samples were p-type and two were n-type. The results of these measurements are shown in Fig. 3 where samples 1 to 4 are p-type and A, B are n-type.

The resulting curves of conductivity and Hall constant variation as a function of 1/T are quite typical of semiconductors. Each conductivity and Hall effect curve possesses a nearly horizontal impurity conduction branch and a nearly vertical intrinsic conduction branch. A reasonable explanation of these curves can be obtained by considering the basic band picture of a semiconductor shown in Fig. 4.

The nearly vertical line between (0 and 5) $10^3/T$, shown in Fig. 3, is in the region where the thermal energy at 200 to 300° K is sufficient to support intrinsic conduction. For

[5] H. Welker, "Semiconducting Intermetallic Compounds", Physica, Vol. 20, pp. 893-909; 1954

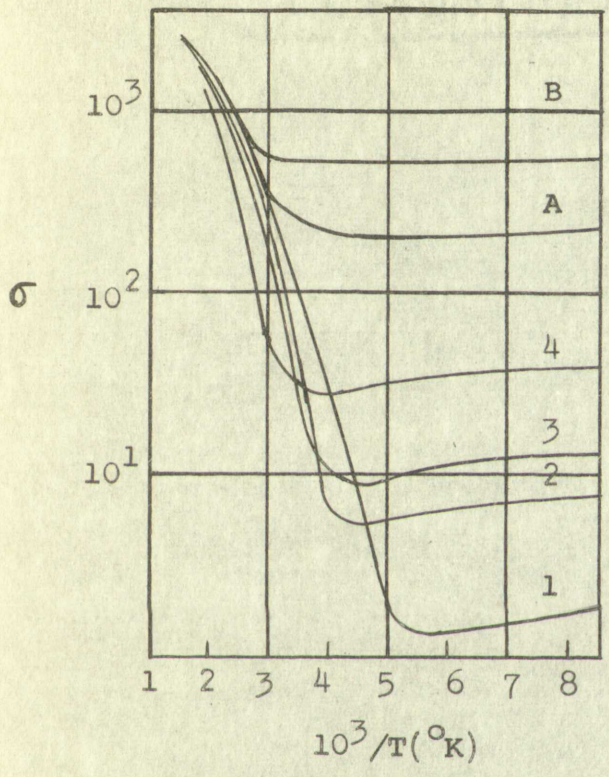

CONDUCTIVITY OF InSb VS $10^3/T(^oK)$

(AFTER H. WELKER)

FIG. 3

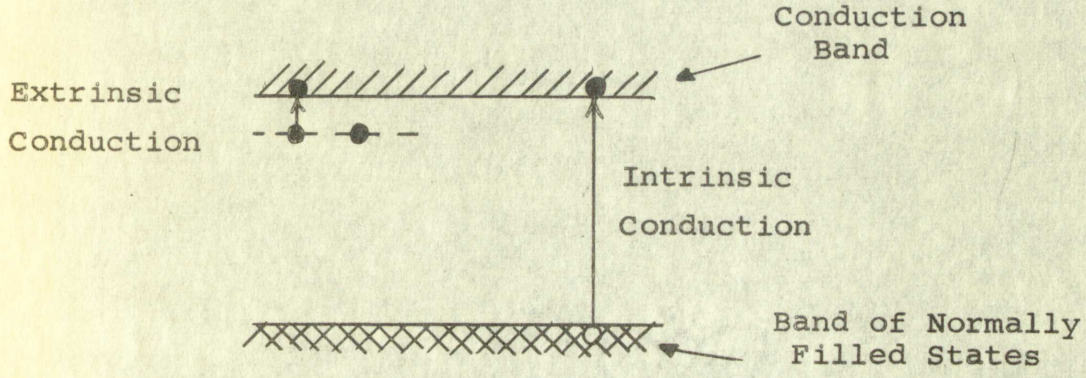

BAND PICTURE OF A SEMICONDUCTOR

FIG. 4

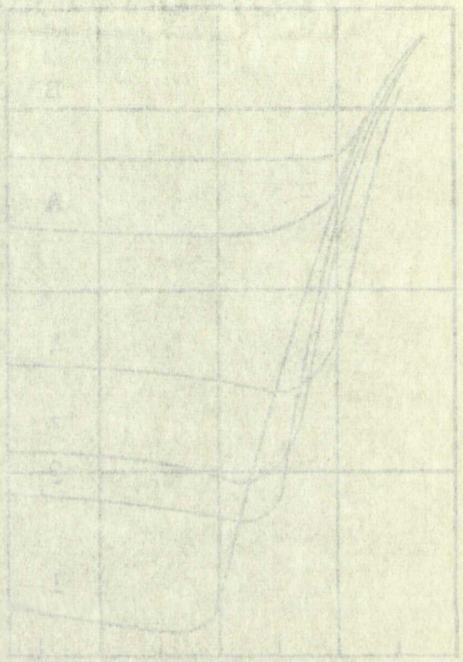
10^3
10^2
10^1
1 2 3 4 5 6 7 8

temperatures in the range of 100 to 200° K the available thermal energy will only support extrinsic or impurity level conduction; thus, for a strongly n-type sample of InSb the impurity level shown in Figure 4 is very close to the conduction band ($\pm$ .01ev difference) and extrinsic conduction predominates. The small variation in conductivity and Hall constant in this range can be explained by the fact that there is more than enough thermal energy available even down to (-196)° C to separate an electron from the impurity level and raise it into the conduction band.

In the experiment performed the temperature of the semiconductor sample ranged over the interval 300 to 400° K and variations in conductivity and Hall constant occurred and were quite pronounced; to account for these changes in conductivity theoretically, it is necessary to derive an expression for conductivity as a function of temperature.

2.321 Derivation of Conductivity Expression. It has been shown that the electrical conductivity[6] in the intrinsic region can be expressed by

$$\sigma_i = 2|e|\left(\frac{2\pi kT}{h^2}\right)^{3/2} (m_e m_h)^{3/4}\, e^{\frac{-E_g}{2kT}} (\mu_e+\mu_h) \qquad (1)$$

where m_e is the effective mass of the electrons and m_h is the effective mass of the hole. The total conductivity of

[6] C. Kittel, Introduction to Solid State Physics, John Wiley Inc., New York, N. Y., 1956, pp. 347-351.

temperatures in the range of 150 to 250° K the ionization
thermal energy will only supply extrinsic or impurity
level conduction; thus for a strongly n-type sample of
InSb the impurity level shown in Figure 6 is very close to
the conduction band (ΔE often different) and extrinsic
conduction predominates. The small variation in conductivity
and Hall constant in this range can be explained by the fact
that there is more than enough thermal energy available even
down to $(-196)^{\circ}$ C to separate an electron from the impurity
level and raise it into the conduction band.

In the experiment performed the temperature of the
semiconductor sample ranged over the interval -150 to 100° F
and variations in conductivity and Hall coefficient obtained
and were quite pronounced. To account for these changes in
conductivity theoretically, it is necessary to derive an
expression for conductivity as a function of temperature.

2.321 Derivation of Conductivity Expression. It has
been shown that the electrical conductivity in the intrinsic
region can be expressed by

$$\sigma_i = 2|e|\left(\frac{2\pi m_e kT}{h^2}\right)^{3/2} \mu_e e^{-\frac{\Delta E}{2kT}}$$

where m_e is the effective mass of the electron and μ_e is
the effective mass of the hole. The total conductivity of

---

[6] C. Kittel, Introduction to Solid State Physics, 3rd Ed.,
Inc., New York, N.Y., 1966, pp. 247-251.

an n-type sample of InSb is the sum of the intrinsic and extrinsic conductivities:

$$\sigma_{total} = \sigma_{int.} + \sigma_{ext.}$$

The total conductivity can be expressed as $\sigma(T) = 50 + \sigma_{int}$ where σ_{ext} was estimated from the experimental value determined at -60° C. To solve equation (1), the following constants were used:

K = Boltzman's constant = $1.38 \times 10^{-16} \frac{ergs}{deg}$ or $8.62 \times 10^{-5} \frac{ev}{deg}$

h = Plancks constant = 6.62×10^{-27} erg sec

e = electron charge = 1.6×10^{-19} coulombs

me = effective electron mass = $.034\ m_o = .31 \times 10^{-28}$ gr.

mh = effective hole mass = $.2\ m_o = 1.82 \times 10^{-28}$ gr.

ue = electron mobility = 50000 cm^2/volt-sec

uh = hole mobility = 2500 cm^2/volt-sec

Eg = band gap energy = .18 electron volts

T = degrees Kelvin

Substituting the previous quantities into equation (1) yields the following expression for intrinsic conductivity as a function of temperature: $\sigma_{int.} = T^{3/2}\ e^{-1044/T}$

Thus, the total conductivity is $\sigma_{total} = 50 + T^{3/2} e^{-1044/T}$.

The theoretical curve for σ_{total} versus $10^3/T$ is shown in Fig. 5 for the Indium Antimonide used by the Halltron. The device was then subjected to four different temperatures,

an n-type sample of InSb is the sum of the intrinsic and
extrinsic conductivities:

$$\sigma_{total} = \sigma_{int} + \sigma_{ext}$$

The total conductivity can be expressed as $\sigma(T) = \sigma_0 + \sigma_1$
where σ_{ext} was estimated from the experimental value
determined at 300°C. To solve equation (1), the following
constants were used:

K = Boltzman's constant
h = Planck's constant
e = electron charge
me = effective electron mass
mh = effective hole mass
ue = electron mobility
uh = hole mobility
Eg = band gap energy
T = degrees Kelvin

Substituting the above numerical values yields the following expression for intrinsic conductivity as a function of temperature:

Thus, the total conductivity is known.

The theoretical curve for σ_{total} versus T is shown in Fig. 5 for the InSb sample used in the device. The device was then subjected to four different temperatures

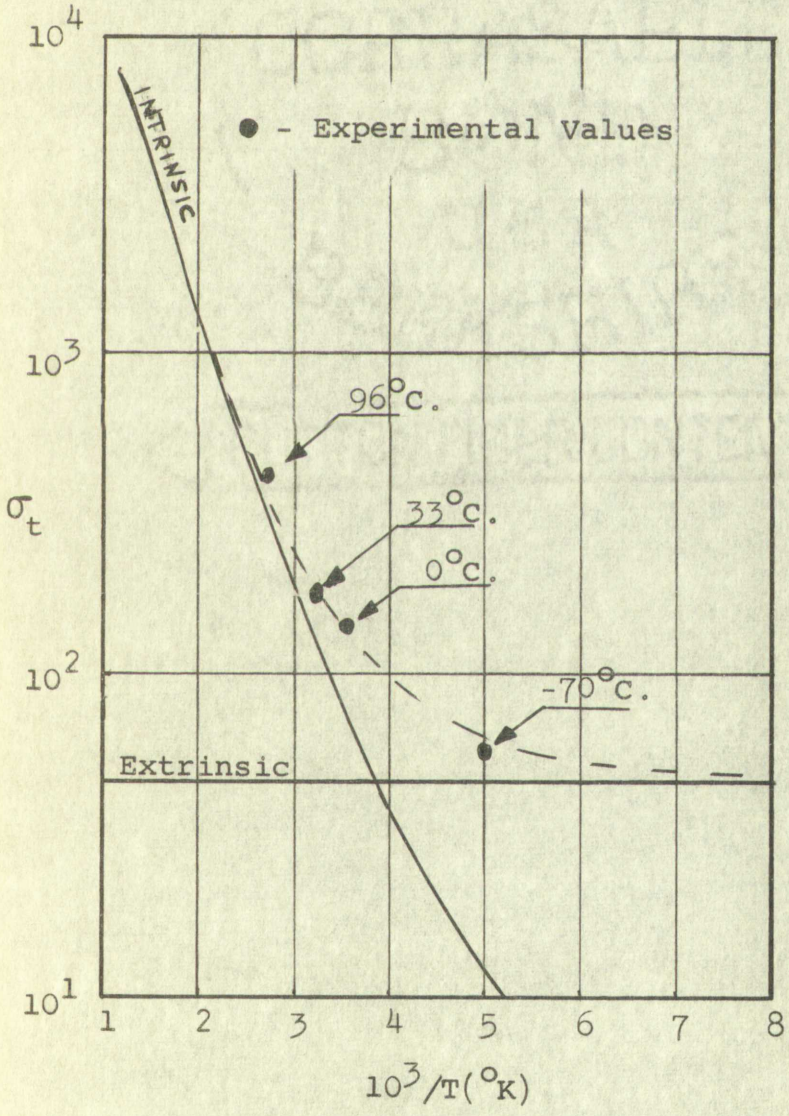

CONDUCTIVITY VS. $10^3/T(^oK)$

For InSb Used by HS-51 Halltron

FIG. 5

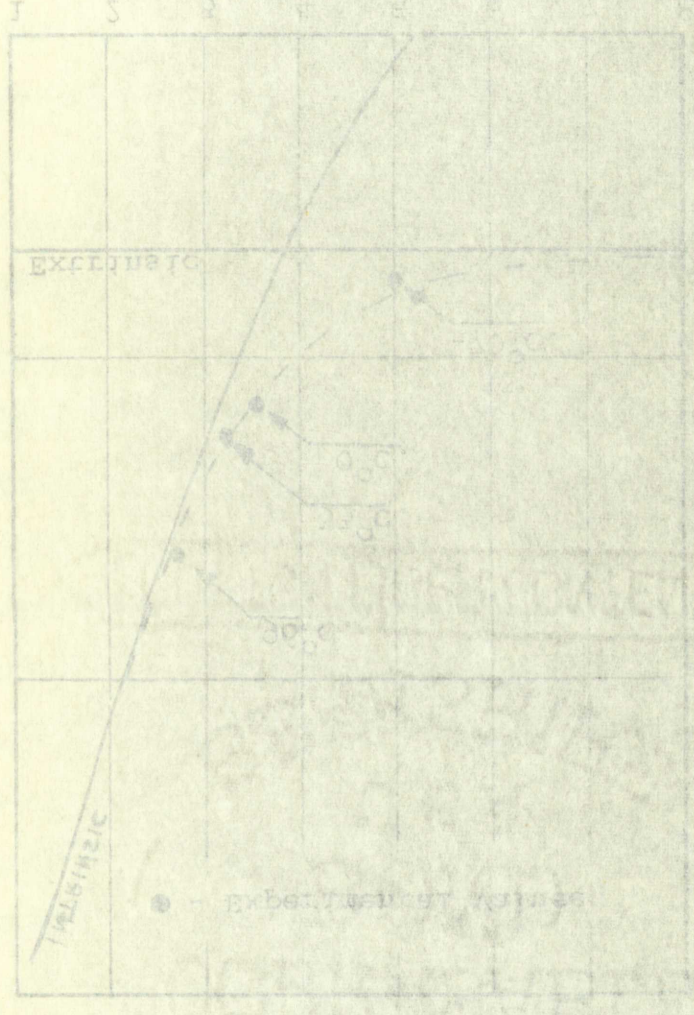

its conductivity measured, and these values added to the curve to check the validity of the expression for σ_{total}.

2.322 Variation of Conductivity with Magnetic Field. The variation of conductivity with magnetic field has been the subject of numerous investigations on semiconductor properties. Sommerfeld[7] showed that there was a small magnetoresistance in metals, arising from the distribution in velocity of electrons. The results were: $\frac{\Delta\rho}{\rho} = \frac{BH^2}{1+\mu^2H^2}$ where B is a constant determined by the effective mass, temperature, mean free path length, etc.

The theory of magnetoresistance for semiconductors was first studied by Harding[8], who also investigated the dependence of the Hall constant on magnetic field.

The magnetoresistance effect in semiconductors is generally thought of in the following way.[9]

If all the electrons were of the same velocity when the magnetic field was applied, a Hall field would be built up just to counteract the Lorentz force, and all the electrons would continue through the crystal with no change in their trajectories. Because of the differing velocities, the Hall field will compensate for the Lorentz force only on the average, to make the net current in the y direction equal to zero. Fast and slow electrons will be deviated one way

---

[7] A. Sommerfeld, Naturwissenschaften, Vol. 22, p. 49, 1934.

[8] J. W. Harding, Proc. Roy. Soc. London, Vol. 140A, p. 205, 1933.

[9] W. C. Dunlap, Jr., An Introduction to Semiconductors, John Wiley Inc., p. 112, 1957.

[7] A. Sommerfeld, Naturwissenschaften, Vol. 2, [illegible]

[8] J. W. Harding, Proc. Roy. Soc. London, Vol. 150A, [illegible]

[9] W. C. Dunlap, Jr., An Introduction to Semiconductors, John Wiley Inc., p. 112, 1957.

or the other. They will suffer more collisions than usual in going the length of the sample, and the mean free path along the sample will thereby be reduced. Harding calculated this effect, assuming the Boltzman's distribution of velocity among the electrons. He found that the resistance of the semiconductor should increase according to the square of the magnetic field. This was true for low fields, but does not necessarily obey the square law for fields greater than 5 kilogauss. Since Harding was hesitant to place an exact variation on the resistance beyond this and others as well, it was decided that an experimental determination of conductivity variation would be made on the device material. This was accomplished by measuring the voltage change across the sample for variations in magnetic field (0 to 22 KG) using .1 milliamp input current. At this low current, the IR heating and other associated heating effects would be held to a minimum. The results of these measurements showed the conductivity decreased with increasing magnetic field according to the relationship $\sigma = \frac{200}{1 + .25 \times 10^{-3} H}$, which is plotted at room temperature and shown in Fig. 6.

Combining the temperature and magnetic field effects, the conductivity can be expressed as

$$\sigma(T, H) = \frac{50(1+.02T^{3/2}e^{-1044/T})}{1 + .25 \times 10^{-3} H}$$

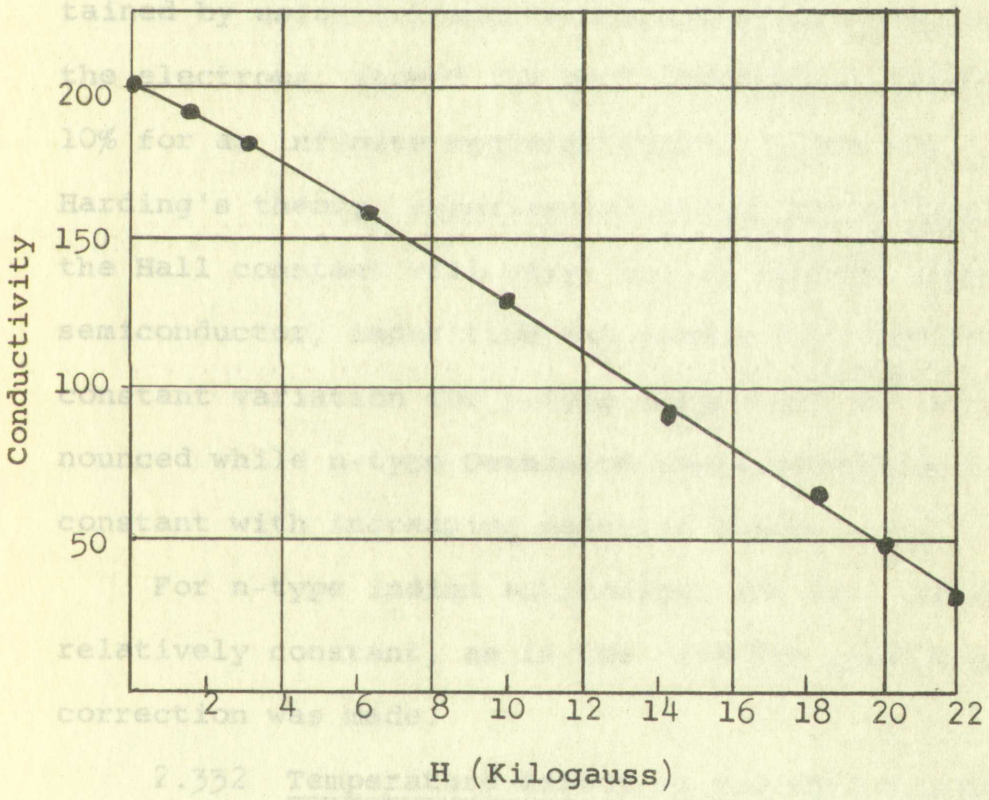

VARIATION OF CONDUCTIVITY WITH MAGNETIC FIELD

FIG. 6

200
150
100
50

2.33 Temperature and Magnetic Field Effect on the Hall Constant

2.331 Magnetic Field Effect on Hall Constant. The variation in Hall constant for different magnetic fields was determined by Harding[10] to be quite small. The results obtained by using Boltzman's distribution of velocity among the electrons, showed the Hall constant to decrease about 10% for an infinite magnetic field. Since the time of Harding's theory, experimental measurements have shown that the Hall constant will vary, but it depends upon the type of semiconductor, impurities and sample temperature. The Hall constant variation for p-type Germanium[11,12] is quite pronounced while n-type Germanium shows no change in the Hall constant with increasing magnetic field.

For n-type indium antimonide, the Hall constant remains relatively constant, as is the case for germanium, and no correction was made.

2.332 Temperature Effect on the Hall Constant. Although the Hall constant change for variations in magnetic field is quite small, the same is not true for temperature variations.

---

[10] J. W. Harding, Proc. Roy. Soc. London, Vol. 140A, p. 205, 1933.

[11] W. C. Dunlap, Jr., Physical Review, Vol. 82, p. 329, 1951.

[12] T. C. Harman, R. K. Willardson, and A. C. Beer, Physical Review, Vol. 96, p. 1512, 1954.

Since the Hall mobility μ_H is related to the drift mobility by the expression $\mu_H = \frac{3\pi\mu}{8}$, and $\mu_H = R\sigma$, then it can be seen that $R = \frac{3\pi}{8}\frac{\mu}{\sigma}$. If the Hall constant is the ratio of mobility/conductivity and the conductivity decreases for increasing magnetic field, then in order for the ratio to remain constant, the mobility must decrease. Since the conductivity is dependent on both magnetic field and temperature, the Hall constant variation should be the inverse to the change in conductivity. The expression for the Hall constant then is

$$R_H = \frac{3\pi}{8}\frac{\mu}{\sigma(T)} \quad \text{or} \quad R_H = \frac{10^3}{1 + .02T^{3/2}e^{-1044/T}}$$

CHAPTER III

EXPERIMENTAL ANALYSIS

A description will be given of the Hall generator used in the experiments. The different types of circuits, methods and problems involved in measurement of voltage gain, current gain, input impedance and output impedance will be discussed.

3.1 Hall Generator Description and its Mounting. The Hall generator used in the experiments was the HS-51 Halltron, produced by Ohio Semiconductors Inc. Fig. 7 illustrates its mechanical construction and dimensions. Indium antimonide, with a mobility of 50000 $\frac{cm^2}{volt\ sec}$, was the semiconductor material used as the active element.

The Hall generator was mounted on a pivoted arm secured to the base mount on the carriage of an electromagnet. This allowed the generator to be moved in and out of the magnetic field. The output and input leads were brought down the pivot arm to two terminals on the base mount as shown in the Fig. 8.

The paint and epoxy material covering the commercial unit was removed from one side and an iron-constantan thermocouple was placed against the exposed surface and held by pressure clamps.

3.2 Instruments Used. A Varian four-inch electromagnet was used to provide the magnetic field. Field intensities

A description will be given of the basic components used in the experiments. The different types of circuits, methods and problems involved in measurement of voltage gain, current gain, input impedance and output impedance will be discussed.

3.1 Hall Generator-Description and Mounting. The Hall generator used in the experiments was the Model [illegible] produced by Ohio Semiconductors Inc. Fig. 7 [illegible] the mechanical construction and dimensions. It has a mobility of 5000 $\frac{cm^2}{volt\text{-}sec}$ when the semiconductor material used as the active element.

The Hall generator was mounted on a [illegible] arm secured to the base mount on the cartridge of an electrometer. This allowed the generator to be moved in and out of the magnet field. The output and input leads were brought down the [illegible] arm to two terminals on the base mount as shown in the Fig. 8.

The paint and epoxy material covering the [illegible] was removed from one side and a [illegible] was placed against the exposed surface and held in pressure clamps.

3.2 Instruments Used. A Weston [illegible] was used to provide the magnetic field. Field intensities

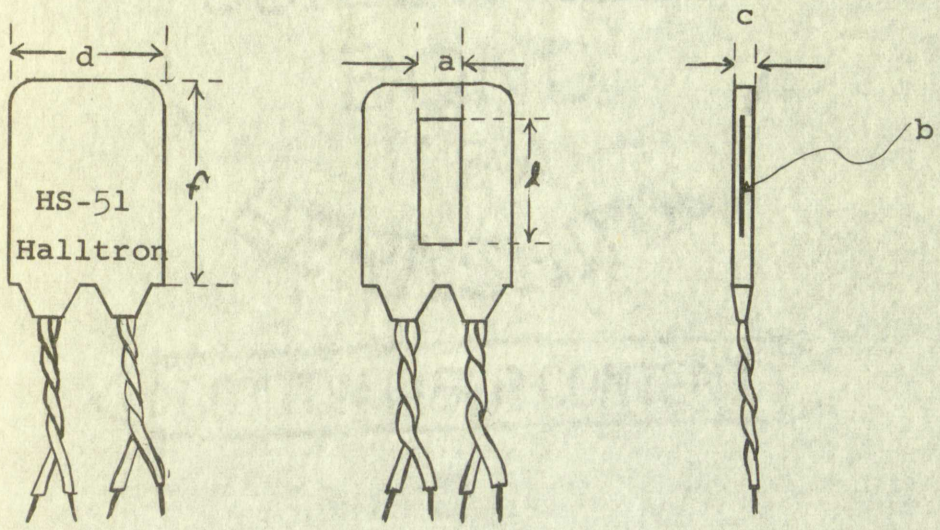

Package Dimensions		Active Element Dimensions	
length f	5/8"	length ℓ	.5"
width d	1/2"	width a	.25"
thickness c	.03"	thickness b	.005"

HS-51 Halltron Dimensions

FIG. 7

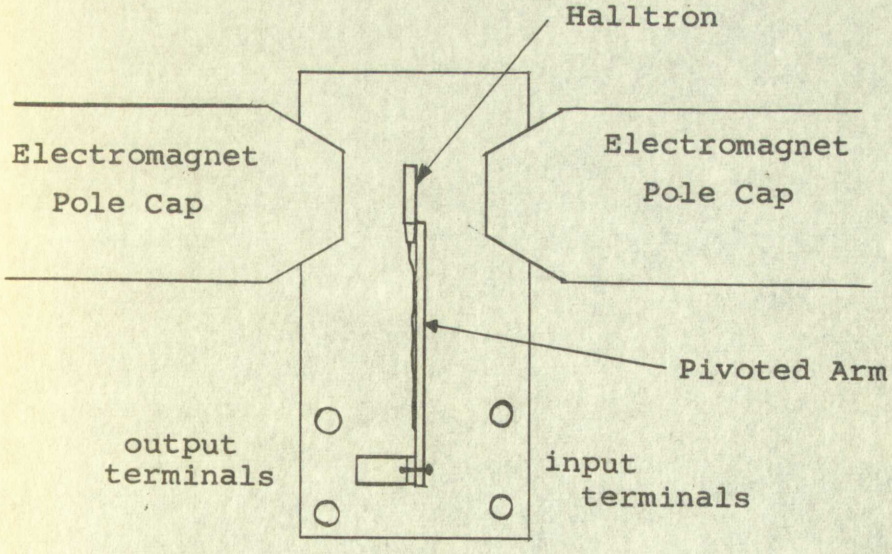

Electromagnet and Hall Generator

FIG. 8

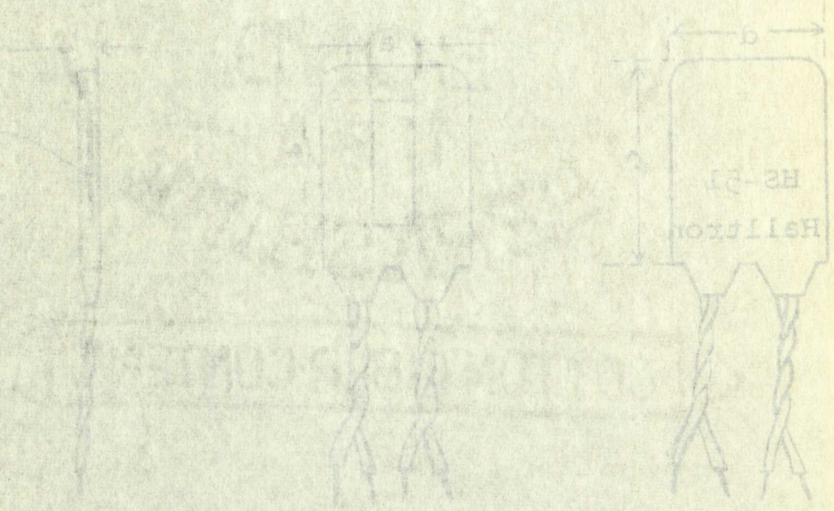

Package Dimensions

length ℓ 5/8"

width d 1/2"

thickness c .05"

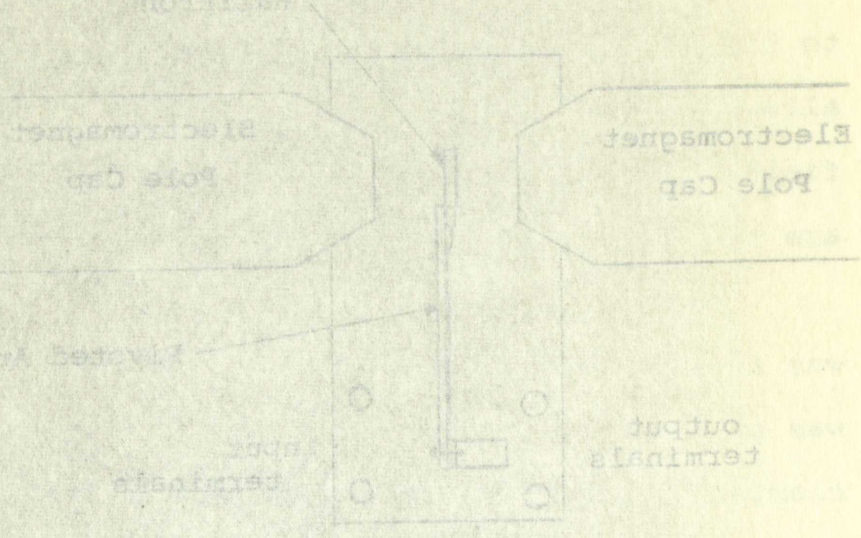

from 0 to 25 kilogauss could be obtained with this system.

A K-2 Leeds and Northrup potentiometer, ranging from 1 microvolt to a maximum 1.6 volts, was used to measure the different voltages associated with the Halltron. To determine the input current a John Fluke differential voltmeter was used to measure the voltage across a standard 10 ohm resistance in the input circuit.

3.3 Circuit Configurations. To obtain experimental data for the current gain, voltage gain, input resistance, and output resistance three circuits were used.

The first circuit, shown in Fig. 9, was constructed so the output would be unloaded. To permit measuring the Hall voltage and input voltage so as to make them correspond with the infinite load case, the input current was monitored by the measurement of voltage drop across the 10 ohm resistor and the input resistance of the device could be determined by the input voltage. From this configuration, data for voltage gain, input resistance for 50 ma and 500 ma input current as functions of magnetic field were obtained.

The second circuit, shown in Fig. 10, was constructed so the output would be loaded as little as possible. Ideally it would be desirable to be able to measure the output current under shorted conditions; however, since conventional current measuring instruments present a prohibitively large

from 0 to 25 kilopases could be treated with this system.

A K-2 Leeds and Northrup potentiometer, reading from 1 microvolt to a maximum 1.6 volts, was used to measure the different voltages associated with the facility. To determine the input current a John Fluke differential voltmeter was used to measure the voltage across a standard 10 ohm resistance in the input circuit.

3.3 Circuit Configurations. To obtain experimental data for the current gain, voltage gain, input resistance and output resistance three circuits were used.

The first circuit, shown in Fig. 5, was connected so the output would be unloaded. To permit measuring the full voltage and input voltage so as to make them correspond with the infinite load case, the input current was monitored by the measurement of voltage drop across the 10 ohm resistor and the input resistance of the device could be determined by the input voltage. From this configuration, data for voltage gain, input resistance for 50 ma and 100 ma input current as functions of magnetic field were obtained.

The second circuit, shown in Fig. 6, was connected so the output would be loaded as little as possible. Ideally it would be desirable to be able to measure the output current under shorted conditions. However, since conventional current measuring instruments present a problem in that they

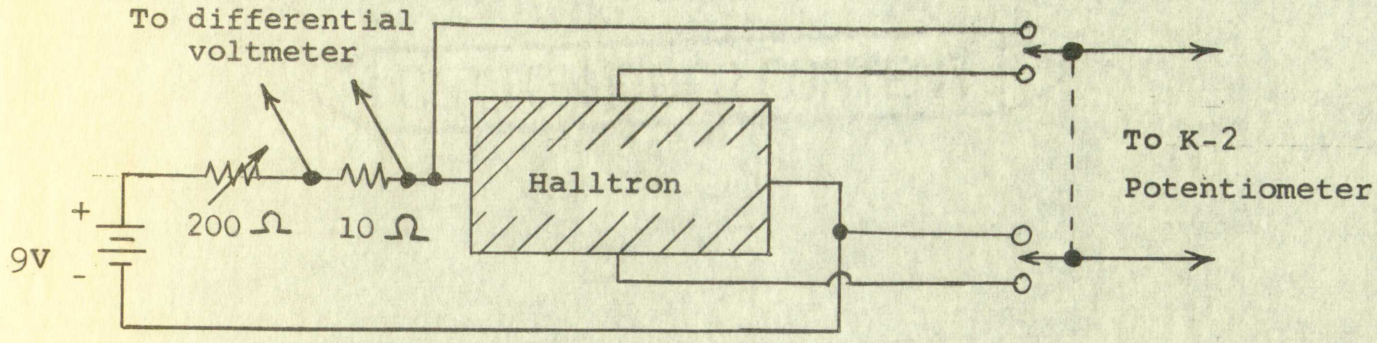

Circuity for measurement of voltage gain and input resistance ($Z_L = \infty$)

FIG. 9

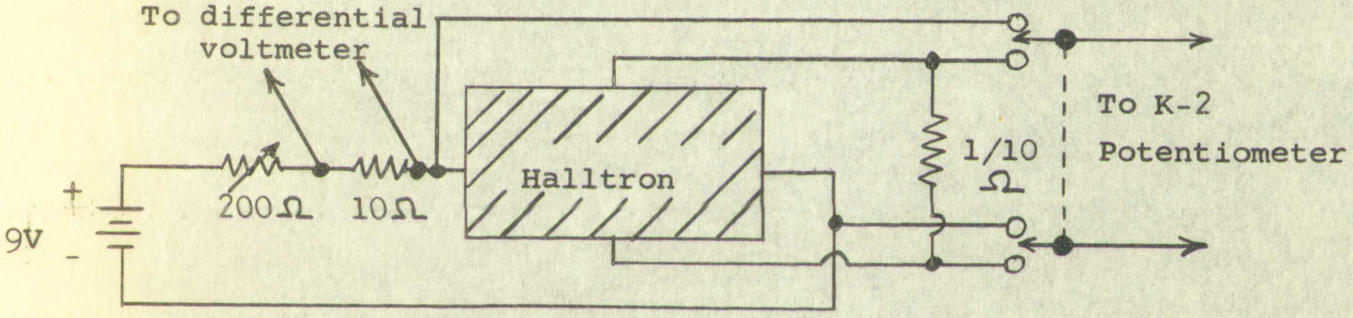

Circuity for measurement of current gain and input resistance ($Z_L \approx 0$)

FIG. 10

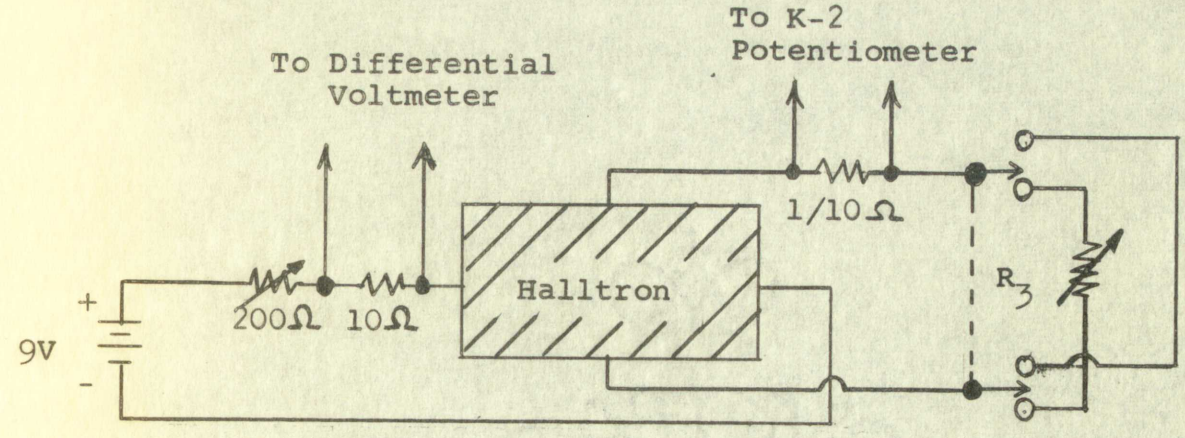

Circuity for measurement of output resistance

FIG. 11

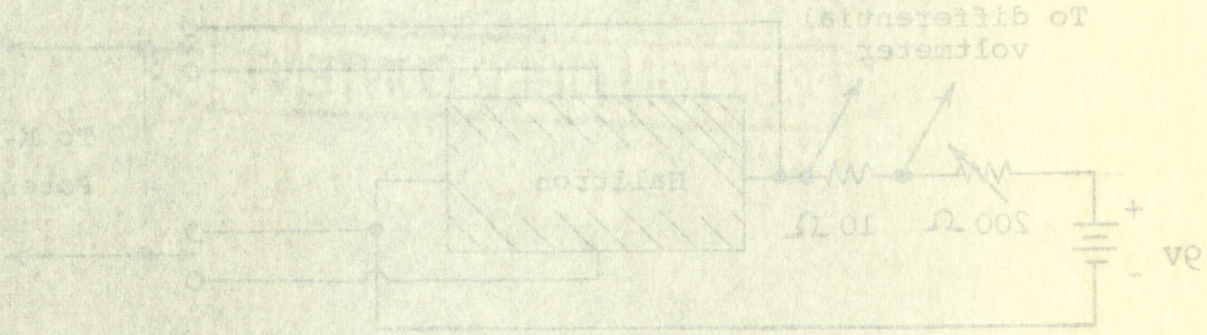

Circuity for measurement of voltage gain and input resistance

FIG. 9

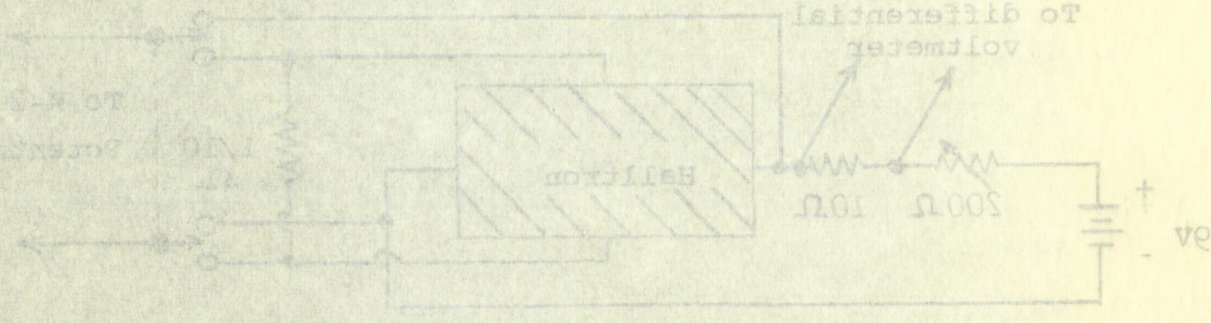

Circuity for measurement of current gain and input resistance

FIG. 10

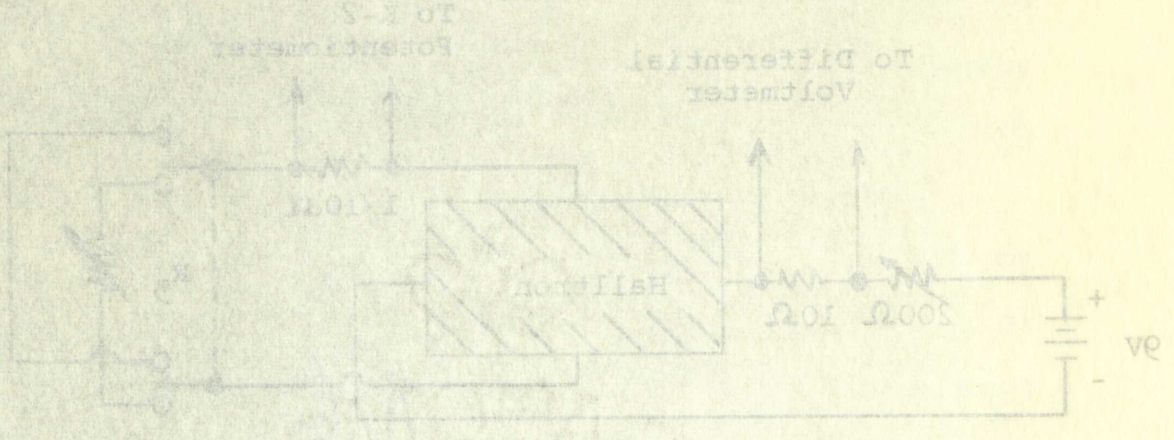

Circuity for measurement of output resistance

FIG. 11

impedance to the circuit, it was necessary to choose a .1 ohm resistance in the output in order to approximate a short circuit and still have a reasonable voltage drop to measure. From the second configuration data was obtained for current gain and input resistance.

The third circuit, shown in Fig. 11, was used to determine output resistance as a function of magnetic field. The input current was held constant (50 and 500 ma) for various field intensities and the voltage across the 1/10 ohm resistor was measured.

3.4 Experimental Procedure. To obtain data for curve plotting the magnetic field was varied in steps of 1.5, 3.0, 6.5, 10.0, 14.5, 18.5, 20.0 and 22.0 kilogauss, with the input current at either 50 or 500 ma. This variation in magnetic field intensity increased the resistance of the sample, thereby reducing the input current. Consequently, it was necessary to readjust the input voltage to keep the current constant. In the open circuit case the Hall output voltage, input voltage, and temperature of the sample were measured after the input current had been readjusted to the constant value.

The third circuit involved the use of a precision variable resistance in the output. The output resistance of the generator had to be measured in a way similar to the

impedance to the circuit, it was necessary to choose a 1
ohm resistance in the output in order to approximate a short
circuit and still have a reasonable voltage drop to measure.
From the second configuration data was obtained for current
gain and input resistance.

The third circuit, shown in Fig. 11, was used to deter-
mine output resistance as a function of magnetic field. The
input current was held constant (50 and 500 ma) for various
field intensities and the voltage across the 1/10 ohm resistor
was measured.

3.4 Experimental Procedure. To obtain data for curve
plotting the magnetic field was varied in steps of 1.5, 3.0,
6.5, 10.0, 14.5, 18.5, 20.0 and 27.0 kilogauss, with the
input current at either 50 or 500 ma. Each variation in
magnetic field intensity increased the resistance of the
sample, thereby reducing the input current. Consequently
it was necessary to readjust the input voltage to keep the
current constant. In the open circuit case the Hall output
voltage, input voltage, and temperature of the sample were
measured after the input current had been readjusted to
the constant value.

The third circuit involved the use of a potentiometer
variable resistance in the output. The output resistance
of the generator had to be measured in a way similar to the

method used in measuring the internal resistance of a battery. The precision resistance could be varied in 1/10 ohm steps up to a maximum of 10 ohms. The input current was set at a constant value (50 or 500 ma) and the magnetic field set at the incremental steps previously mentioned. At each setting of the magnetic field, the precision resistor (R_3) was shorted across and the voltage across the 1/10 ohm resistor was measured. The short was then removed and R_3 varied until the voltage across R_1 was 1/2 the voltage for the short circuited case.

Mathematically if e is the generated voltage across the Halltron, then for R_3 shorted:

$$I_1 = \frac{e}{R_1 + R_x}$$

where R_1 is 1/10 ohm and R_x the unknown output resistance. When the short is removed, there flows a different current, namely, $I_2 = \frac{e}{R_1 + R_3 + R_x}$. R_3 was then varied until the voltage across R_1 was 1/2 of the previous voltage. This meant that $I_2 = \frac{I_1}{2}$ and substituting $I_2 = \frac{I_1}{2}$ for I_2,

$$I_1 = \frac{2e}{R_1 + R_3 + R_x} = \frac{e}{R_1 + R_x}$$

Cancelling e from the two equations,

$$2R_1 + 2R_x = R_1 + R_3 + R_x \text{ or } R_x = R_3 - R_1.$$

The output resistance is then the resistance read on the precision resistor minus 1/10 ohm.

CHAPTER IV

THEORETICAL ANALYSIS

A Hall generator is a four-terminal device that uses a magnetic field to couple the input and output; it is similar to simple four-terminal transformer in that the coupling is accomplished by the changing flux which produces a voltage across the secondary coil. The transformation of input energy to the output of a Hall device is accomplished by the application of a transverse magnetic field. Although the mechanism by which an output signal is produced is quite different for the two systems, the result is very similar. In the case of a transformer the output voltage is dependent on the product of the amount of coupling and the rate of change in input current. The output voltage for a Hall generator is a function of the product of input current and the magnetic field.

CHAPTER IV

TYPE-BASED ANALYSIS

A Hall generator is a four-terminal device that uses a magnetic field to couple the input and output. It is similar to simple four-terminal transformers in that the coupling is accomplished by the changing flux which produces a voltage across the secondary coil. The transformation of input quantity to the output of a Hall device is accomplished by the application of a transverse magnetic field. Although the mechanism by which an output signal is produced is quite different for the two systems, the result is very similar. As in the case of a transformer the output voltage is dependent on the product of the amount of coupling and the rate of change in input current. The output voltage for a Hall generator is a function of the product of input current and the magnetic field.

One of the primary differences in the two systems is that a Hall generator will respond to DC and AC input signals while the transformer responds only to AC.

4.1 Four-Terminal Treatment. The theoretical analysis of a Hall generator can be accomplished by using a four-terminal treatment. Four pole systems can vary and can be classified under the following general headings:

UNILATERAL SYSTEM. One-way transmission of an input signal, i. e., only one side of the four-terminal device may be energized and get an output. A vacuum tube is an example of a unilateral device.

BILATERAL SYSTEM. Two-way transmission of a signal, i.e., both sides of the device may be energized and an output will occur on the opposite side of the device. An RC filter is an example of a bilateral device.

RECIPROCAL SYSTEM. Transfer impedances are equal, i.e., if the input terminals are designated (i) and output (o) then $R_{io}(e) = R_{oi}(e)$ where (e) is an independent variable such as frequency, magnetic field, temperature, etc.

NON-RECIPROCAL SYSTEM. Transfer impedances are unequal, i.e., $R_{io}(e) \neq R_{oi}(e)$.

From the preceding classifications a Hall generator may be regarded as a non-reciprocal bilateral device and will be treated as such in the analysis.

To analyze a Hall sample it is necessary to establish firmly the appropriate directions of input current, applied magnetic field, and output field in order that the proper relationship for the assumed sign conventions can be maintained. The four pole equations for the voltage and current relationships shown in Fig. 12 are:

$$V_x = I_x Z_{11} + I_h Z_{12} \qquad (1)$$

$$V_h = I_h Z_{22} + I_x Z_{21} \qquad (2)$$

where Z_{11} and Z_{22} are driving point impedances and Z_{12} and Z_{21} are transfer impedances. In terms of the impedance parameters, if terminals 1 and 1' are energized first and terminals 2 and 2' are left open, then $I_h = 0$ and from equations (1) and (2) $Z_{11} = \left.\frac{V_x}{I_x}\right|_{I_h = 0}$ (3)

and $Z_{21} = \left.\frac{V_h}{I_x}\right|_{I_h = 0}$

Energizing terminals 2 and 2' with terminals 1 and 1' left open so $I_x = 0$, then

$$Z_{22} = \left.\frac{V_h}{I_h}\right|_{I_x = 0} \qquad (4)$$

and

$$Z_{12} = \left.\frac{V_x}{I_h}\right|_{I_x = 0}$$

The properties of a bilateral device insure that Z_{21} and $Z_{12} \neq 0$ and they may be theoretically and experimentally determined.

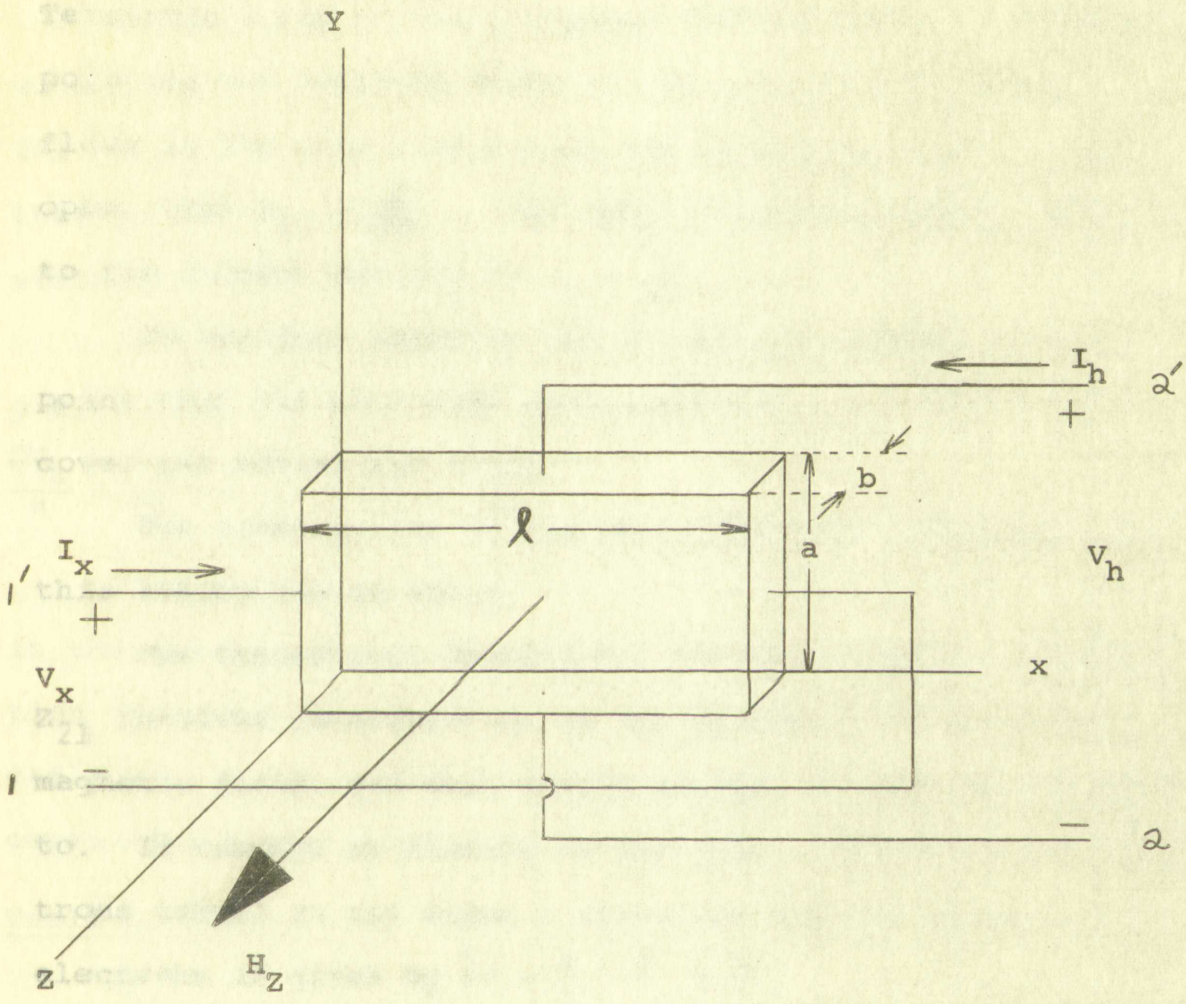

THEORETICAL SLAB USED IN FOUR TERMINAL ANALYSIS

FIG. 12

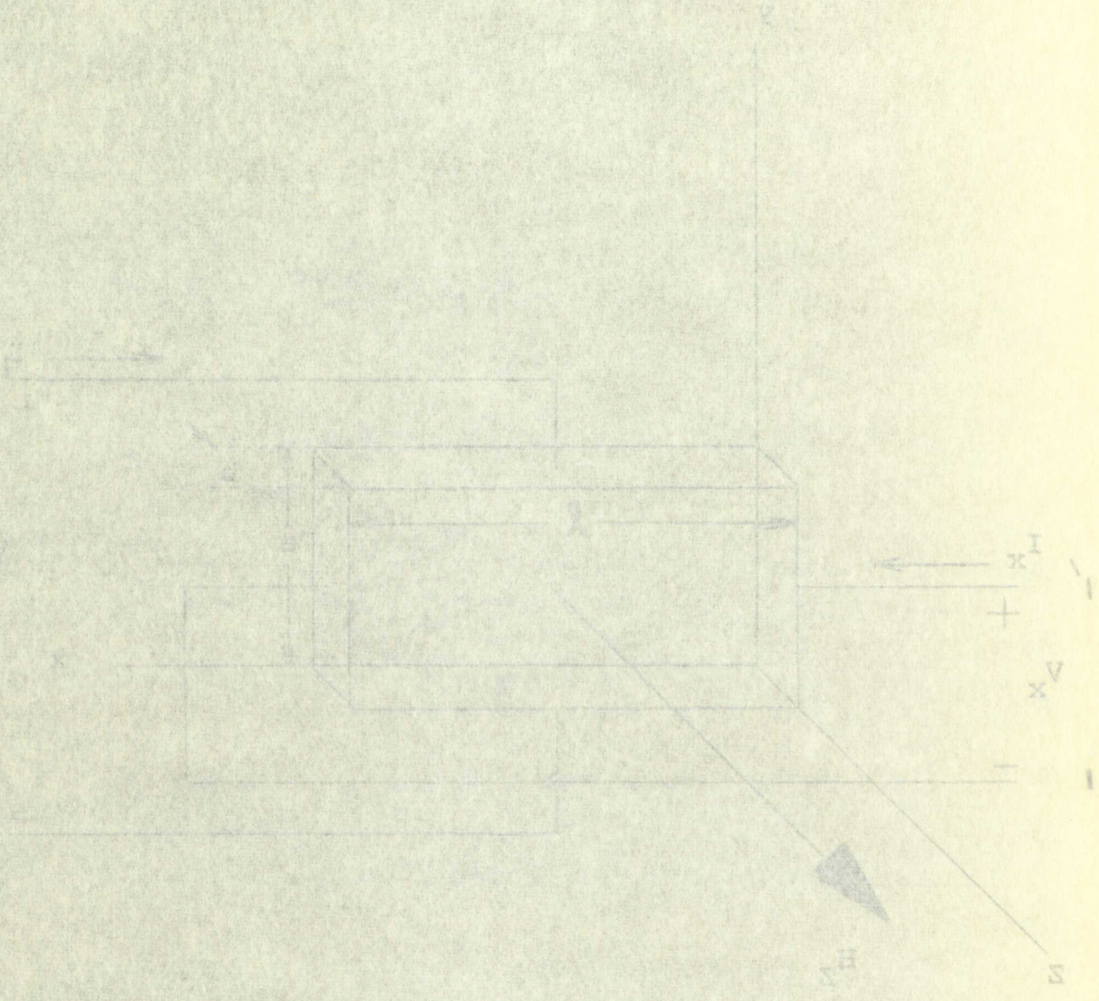

Terminals 1 and 1' are energized commensurate with voltage polarity and currents shown in Fig. 12, so that current flows in the plus x direction and terminals 2 and 2' left open, then $Z_{11} = \frac{\ell}{\sigma ab}$. The total current I_x being related to the current density by $i_x = \frac{I_x}{ab}$.

To validate equation (3) it must be assumed at this point that the electrode attachments at $x = 0$ and $x = \ell$ cover the entire end faces.

The construction of the HS-51 Halltron indicates that this assumption is valid.

The theoretical development for the transfer impedance Z_{21} involves consideration of the direction of electron flow, magnetic field, and Hall fields so Fig. 12 will be referred to. If current is flowing in the plus x direction the electrons travel in the minus x direction and the force on the electrons is given by $\vec{F} = \frac{e}{c} (-\vec{v} \times \vec{H})$.

The cross product $-v_x \times H_z$ is represented by

$$\begin{vmatrix} i & j & k \\ -v_x & 0 & 0 \\ 0 & 0 & +H_z \end{vmatrix} = +v_x H_z \bar{j} = F$$

Considering e a minus quantity for an electron, then the electrons experience a force in the minus y direction and thus support the sign convention in Fig. 12. Knowing that the Hall voltage $V_h = \frac{RI_x H}{b}$ then $Z_{21} = \frac{V_h}{I_x} = \frac{RH}{b}$

To obtain Z_{12} and Z_{22} terminals 2 and 2' are energized with 1 and 1' left open. For the time being if we assume 2-2' electrodes cover the entire end faces (an assumption that is not valid but can be treated as such) and then re-evaluated, then $Z_{22} = \frac{V_h}{I_h}$.

If $I_h = i_h b\ell$ where i_h is the current density in the y direction and $i_h = \sigma E_h$; then if $\frac{V_h}{a} = E_h$, $i_h = \frac{\sigma V_h}{a}$ and $\frac{\sigma V_h}{a} = \frac{I_h}{b\ell}$ or $\frac{V_h}{I_h} = Z_{22} = \frac{a}{\sigma b\ell}$.

If 2-2' terminals are energized so that current flows in the minus y direction or electrons in the plus y direction the cross product $v \times H_z$ causes the electrons to be deflected to terminal 1 of 1-1' in opposition to the sign convention established; thus, $V_x = \frac{-RI_h H}{b}$ and $\frac{V_x}{I_h} = Z_{12} = -\frac{RH}{B}$

Table of Theoretical Driving Point and Transfer Impedances

Z_{11}	Z_{22}	Z_{12}	Z_{21}
$\frac{\ell}{\sigma^* ab}$	$\frac{a}{\sigma^* b\ell}$	$-\frac{RH}{b}$	$\frac{RH}{b}$

σ^* not corrected for temperature and magnetic field

4.2 Theoretical Derivation for Z_{22}. Z_{22} was determined on the basis that the electrodes were area type and in particular covered the entire end faces at y = o and y = a. However the Halltron, or any other Hall generator aspiring to achieve a respectable Hall output voltage, uses point electrodes

rather than area electrodes for one set of terminals. This difference requires a correction for the expression Z_{22} in the four-terminal parameters.

There are several methods for solving a problem of this type, and probably the most used is the solution of Laplace's equation. However, a simpler method will be employed in this paper. An infinite half plane was chosen as a reference plane. The original configuration and desired configuration were then transformed by means of appropriate transformation equations, making it possible to relate original and desired configuration mathematically. The resistance could then be calculated quite easily from the final figure.

There are several assumptions that will be made at this time in order that the analysis be applicable. They are:

1. The width of the contact strip is small compared to the length of the sample; i.e., an infinite slab may be considered.

2. The thicknesses of the contact strip and the sample are essentially the same; i.e., a two dimensional case.

3. Plate contact strips are parallel.

An illustration of the configuration to be transformed is shown in Fig. 13, where k is the width of the contact strip.

Points $(0,i\ell)$, $(K,i\ell)(o,o)$ and $(K,0)$ in the Z_3 plane will be required to map into points (a,o), (b,o), $(-a,o)$, $(-b,o)$ respectively of the Z_2 plane shown in Fig. 14.

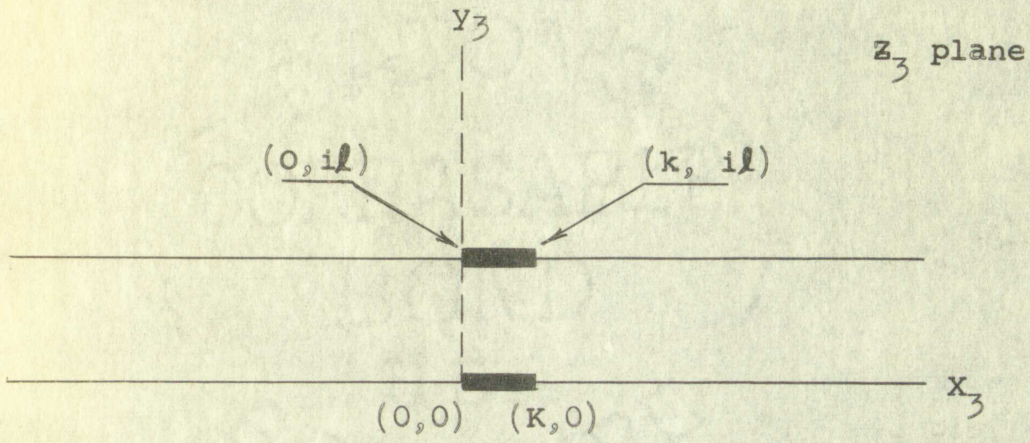

FIG. 13

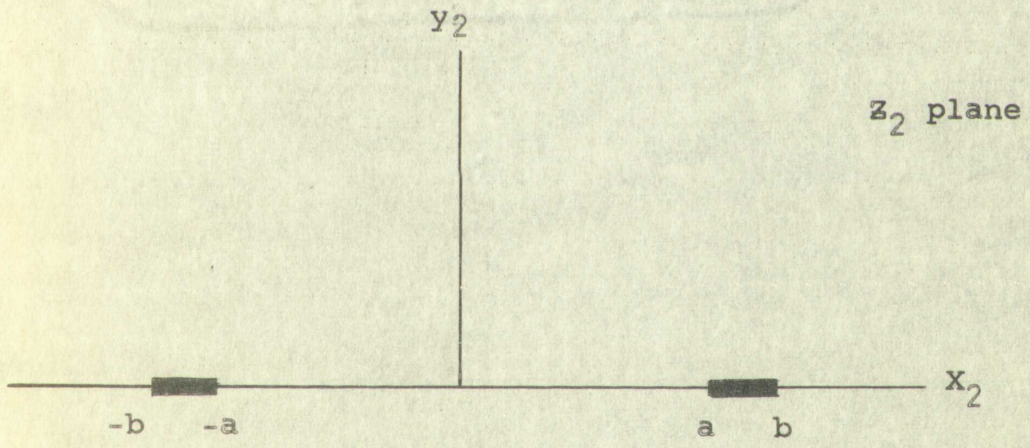

FIG. 14

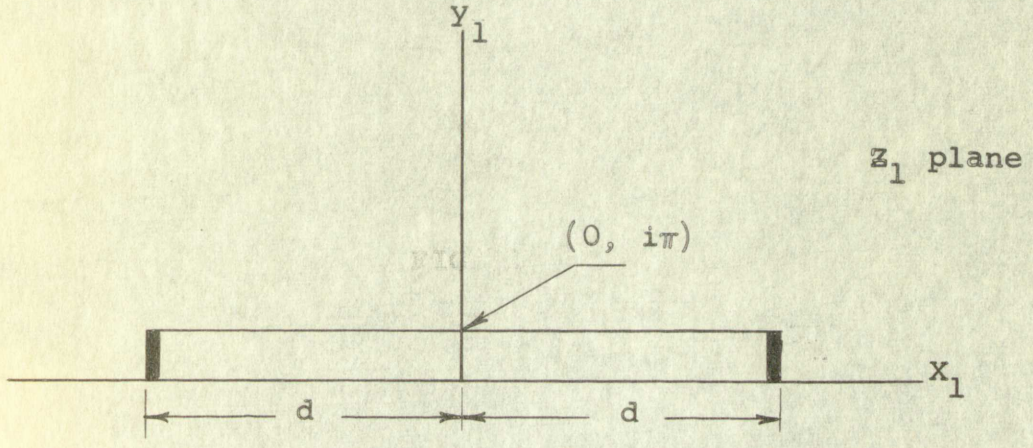

FIG. 15

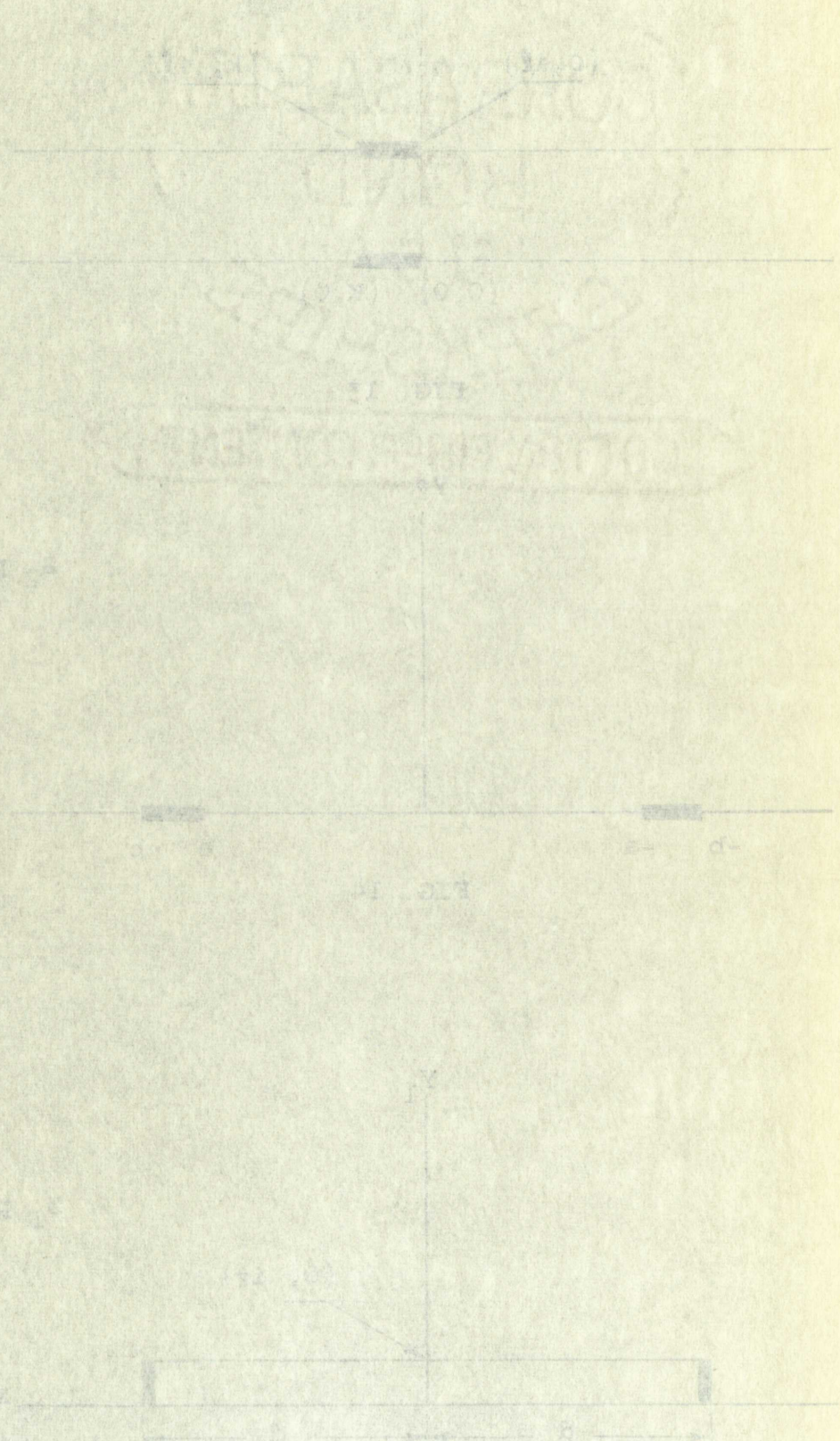

This can be accomplished by considering the transformation $Z_2 = Ke^{CZ_3}$ where K and C are arbitrary constants to be chosen for the required transformation.

Letting $K = a$ and $C = \frac{\pi}{\ell}$

$$Z_2 = ae^{\frac{\pi Z_3}{\ell}}$$

If $Z_3 = 0$, then $Z_2 = a$, and if $Z_3 = i\ell$ then $Z_2 = -a$; thus, points 0 and $i\ell$ of Z_3 have been mapped into points a and -a of Z_2 plane.

For the point $(K, i\ell)$, $Z_2 = ae^{\frac{\pi}{\ell}(i\ell+K)}$, which is $-ae^{\pi k/\ell}$ and we require that $(K, i\ell)$ map into -b of Z_2 plane; then $-b = -ae^{\pi k/\ell}$.

Letting point k be transformed, it can be seen that $b = ae^{\pi k/\ell}$; thus, points $(K, i\ell)$ and (k, o) have been mapped into -b and b.

The next transformation will be made from the infinite half plane into a simple rectangular strip where the resistance may be calculated by the formula $R = \frac{2d}{\sigma \pi t}$ where 2d is the length of the strip, s is the cross sectional area, πt, and σ is the conductivity. Configuration is shown in Fig. 15.

The rectangular bar shown in Fig. 15 can be transformed into the infinite half plane by using the general Schwarz transformation. This transformation (see Appendix II) will reduce any number of rectilinear boundaries of one plane to a single line boundary of another plane.

This can be accomplished by selecting the transformation

$z_2 = Ke^{cz_3}$ where K and c are arbitrary constants to be chosen for the required transformation.

Letting $K = a$ and $c = \frac{\pi}{k}$

$$z_2 = ae^{\frac{\pi z_3}{k}}$$

If $z_3 = 0$, then $z_2 = a$, and if $z_3 = jk$ then $z_2 = -a$; thus points 0 and ik of z_3 have been mapped into points a and -a of z_2 plane.

For the point (K, ik), $z_2 = ae^{\frac{\pi}{k}(x+jk)}$, which is $-ae^{\frac{\pi x}{k}}$ and we require that (K, ik) map into $-b = -ae^{\frac{\pi k}{k}}$.

Letting point x be transformed, it can be seen that $b = ae^{\frac{\pi k}{k}}$; thus, points (K, ik) and (K, o) have been mapped into -b and b.

The next transformation will be made from the half-strip half plane into a simple rectangular strip where the resistance may be calculated by the formula $S = \frac{2d}{\sigma\tau}$ where 2d is the length of the strip, s is the cross sectional area, σ and τ is the conductivity. Configuration is shown in Fig. 15.

The rectangular pair shown in Fig. 13 can be transformed into the infinite half plane by using the general schwartz transformation. This transformation (see Appendix I) will reduce any number of rectilinear boundaries of one plane to a single line boundary of another plane.

The Schwarz transformation[12] is given by the differential equation:

$$\frac{dZ_1}{dZ_2} = C_1 \prod_{i=1}^{n} (Z_2 - ai)^{(\alpha i/\pi)-1}$$

where a_i is the point mapped from the Z_2 plane and αi the angles at corners of polygon in the Z_1 plane. The rectangle of Fig. 15 contains 90° angles; thus $\alpha_i = \frac{\pi}{2}$ and the points mapped from the Z_2 plane are a_1 = a, -a, b, -b. The product

$\prod_{i=1}^{n} (Z_2 - a_i)^{(\alpha i/\pi)-1}$ becomes

$$(Z_2-a)^{-1/2}(Z_2+a)^{-1/2}(Z_2-b)^{-1/2}(Z_2+b)^{-1/2}$$

or

$$\frac{dZ_1}{dZ_2} = \frac{C_1}{\sqrt{(Z_2^2-a^2)(Z_2^2-b^2)}} = \frac{C_1}{\sqrt{Z_2^4-(a^2+b^2)Z_2^2+a^2b^2}}$$

integrating $$Z_1 = \int \frac{C_1 dZ_2}{\sqrt{Z_2^4-(a^2+b^2)Z_2^2+a^2b^2}} + D_1 \qquad (1)$$

where D_i is an arbitrary constant of integration and C_1 the scale factor giving both relative scale and relative angular orientation of the two geometries.

---

[12] W.K.H. Panofsky, Classical Electricity and Magnetism, Addison-Wesley Publishing Co., Reading, Mass., p. 59, 1955.

Integrating expression (1) gives

$$Z_1 = C_1 \log \left[\frac{2\sqrt{z_2^4-(a^2+b^2)z_2^2+a^2b^2}+2z_2^2-(a^2+b^2)}{2} \right] + D_1$$

If it is required that the origin of Z_1 plane map into the origin of Z_2 plane, D_1 may be evaluated at $Z_1 = 0$ and $Z_2 = 0$,

$$0 = C_1 \log \left(\frac{2ab-a^2-b^2}{2} \right) + D_1$$

then

$$D_1 = -C_1 \log \left(\frac{2ab-a^2-b^2}{2} \right)$$

and

$$Z_1 = C_1 \log \left[\frac{2\sqrt{z_2^4-(a^2+b^2)z_2^2+a^2b^2} + 2z_2^2 -(a^2+b^2)}{2ab-a^2-b^2} \right]$$

C_1 may now be evaluated by considering what points of Z_1 map into Z_2. If $Z_1 = d$ and $Z_2 = a$, then

$$d = C_1 \log \frac{a^2-b^2}{-(a-b)^2} = C_1 \log \frac{a+b}{b-a}$$

At $Z_1 = d+i\pi$ and $Z_2 = b$, then

$$d+i\pi = C_1 \log \frac{b^2-a^2}{-(a-b)^2} = C_1 \log \frac{a+b}{a-b}$$

$C_1 \log \frac{a+b}{a-b}$ can be rewritten as

$$C_1 \log \frac{a+b}{b-a} e^{i\pi} = C_1 \log \frac{a+b}{b-a} + C_1 i\pi, \text{ thus}$$

$$d+i\pi = C_1 \log \frac{a+b}{b-a} + C_1 i\pi \text{ and } C_1 = 1.$$

The transformation becomes

$$Z_1 = \log \left[\frac{2\sqrt{Z_2^4-(a^2+b^2)Z_2^2+a^2b^2} + 2Z_2^2-(a^2+b^2)}{-(a-b)^2} \right]$$

with $d = \log \frac{b+a}{b-a}$.

The resistance of the rectangular bar in the Z_1 plane is $R = \frac{2d}{\sigma \pi t}$ where 2d is the length and t is the thickness. Substituting for d, $R = \frac{2 \log}{\sigma \pi t} \left(\frac{b+a}{b-a}\right)$. From the first transformation $b = ae^{\pi k/\ell}$ where k is the width of contact strip and ℓ is width of sample, R then becomes

$$\frac{2 \log}{\sigma \pi t} \quad \frac{e^{\pi k/\ell}+1}{e^{\pi k/\ell}-1}$$

where $\sigma = 200 \text{ ohm}^{-1}\text{cm}^{-1}$
$k = .005$ inches
$\ell = .125$ inches
$t = .005$ inches

Substituting the values for k, ℓ, t, and σ into the expression for the derived resistance

$$R = \frac{2 \log}{7.4} \quad \frac{e^{\pi/25}+1}{e^{\pi/25}-1} = .8 \text{ ohms.}$$

Comparing the resistance derived by the preceding method to the resistance obtained by substituting in the expression $R = \frac{a}{\sigma b \ell} = \frac{1}{10}$, it can be seen that an appreciable difference

exists between the two answers. That is, the point contact electrode increases the resistance by eight times.

$$R = \frac{a}{\sigma b \ell} = .1 \text{ ohms}$$

$$R = \frac{2}{\sigma \pi t} \log \frac{e^{\pi k/\ell}+1}{e^{\pi k/\ell}-1} = .8 \text{ ohms}$$

Applying this correction to the expression for Z_{22} results in $Z_{22} = \frac{8a}{\sigma b \ell}$

Using the corrected value for Z_{22}, the parameters are:

Z_{11}	Z_{22}	Z_{12}	Z_{21}
$\frac{\ell}{\sigma ab}$	$\frac{8a}{\sigma b \ell}$	$\frac{-RH}{b}$	$\frac{RH}{b}$

4.3 **Hall Generator Equations**. The terminal characteristics for a four-terminal device are:

$$Z_{in} = \text{input impedance} = \frac{\Delta^Z + Z_{11}Z_L}{Z_{22}+Z_L}$$

$$Z_o = \text{output impedance} = \frac{\Delta^Z + Z_{22}Z_g}{Z_{11}+Z_g}$$

$$A_v = \text{voltage gain} = \frac{Z_{21}Z_L}{\Delta^Z + Z_{11}Z_L}$$

$$A_i = \text{current gain} = \frac{-Z_{21}}{Z_{22}+Z_L}$$

where $\Delta^Z = Z_{11}Z_{22} - Z_{12}Z_{21}$. Substituting for Z_{11}, Z_{22}, Z_{12}

exists between the two squares. That is, the coin tosser

electrode increases the resistivity eight times.

$$R = \frac{\rho}{a} \Omega$$

$$R = \frac{2}{\pi} \ln \frac{}{}$$

Applying this correction to the expression for Z_{22}

results in $Z_{22} =$

Using the corrected value for Z_{22}, the parameters

$$\frac{Z_{11}}{\sigma ab}$$

4.5 Ratio Generator Equations. The terminal characteristics for a four-terminal device are:

Z_{in} = input impedance =

Z_o = output impedance =

A_v = voltage gain =

A_i = current gain =

where $\Delta_z = Z_{11}Z_{22} - Z_{12}Z_{21}$; substituting for

and Z_{21} the expressions for Z_{in}, Z_o, A_v, and A_i reduce to

$$Z_{in} = \frac{\ell}{\sigma ab}\left(1 + \frac{R^2H^2\sigma^2 a}{8a+\sigma b\ell Z_L}\right)$$

$$Z_o = \frac{a}{\sigma b\ell}\left(8 + \frac{R^2H^2\sigma^2\ell}{\ell+\sigma abZ_g}\right) \qquad (6)$$

$$A_v = \frac{+RH\sigma^2 abZ_L}{a(8+R^2H^2\sigma^2)+\sigma b\ell Z_L}$$

$$A_i = \frac{+RH\sigma\ell}{8a+\sigma b\ell Z_L}$$

The above equations have not been corrected for the variation of conductivity $\sigma(T,H)$ with temperature and magnetic field.

The conductivity variation with temperature and magnetic field determined earlier was shown to be

$$\sigma = \frac{50(1+.02T^{3/2}e^{-1044/T})}{1 + .25 \times 10^{-3}H}$$

while the Hall constant was $R_H = \frac{10^3}{1+.02T^{3/2}e^{-1044/T}}$

Substituting $R_H(T)$ and $\sigma(T,H)$ in equations (6), the final Hall generator equations are:

and Z_{21} the expressions (or ξ_{in}, ξ_o, λ_v and λ_t reduce to

$$Z_{in} = \frac{\ell}{\alpha ab}\left[\beta + \frac{(c^2H^2a)10^{-16}}{8a\beta + b\ell Z_L\alpha}\right]$$

$$Z_o = \frac{a}{\alpha b\ell}\left[8\beta + \frac{(c^2H^2a)10^{-16}}{\beta\ell + \alpha abZ_g}\right]$$

$$A_i = \frac{(CH\ell)10^{-8}}{8a\beta + \alpha b\ell Z_L}$$

$$A_v = \frac{(CH\alpha abZ_L)10^{-8}}{a\left[8\beta + (c^2H^2)10^{-16}\right] + \alpha\beta b\ell Z_L}$$

where $\beta = 1 + .25 \times 10^{-3}H$

$\alpha = 50(1 + .02T^{3/2}e^{-1044/T})$

$C = 5 \times 10^4$

H = Magnetic field in Kilogauss

Z_L = Load impedance

Z_g = Generator impedance

a = Width of Hall sample

b = Thickness of Hall sample

ℓ = Length of Hall sample

$$Z_{in} = \frac{\rho}{c(ab)} \left[\frac{\beta + \frac{(c^2 x^2 a) 10^{-12}}{B a \beta + b k z_L^2 \rho c}}{} \right]$$

$$Z_o = \frac{a}{c(b\chi)} \left[B\beta + \frac{(c^2 x^2 a) 10^{-12}}{\beta\chi + a c a b k^2} \right]$$

$$A_I = \frac{(CR\chi) 10^{-6}}{B a \beta + a b k z_L^2}$$

$$A_V = \frac{(CBk\beta z_L^2) 10^{-8}}{a\left[B\beta + (c^2 R^2) 10^{-10}\right] + a c b k z_L^2}$$

where $\beta = 1 + .25 \times 10^{-2}$

$\alpha = 50(1 + .02\pi)^{2/2} - 10^{-4}$

$C = 5 \times 10^{-4}$

B = Magnetic field in kilogauss

Z_L = Load impedance

Z_g = Generator impedance

a = Width of rail in cm

b = Thickness of armature

β = Length of rail armature

CHAPTER V

PROPERTIES OF HALL GENERATOR

5.1 Results of a Theoretical and Experimental Analysis. The equations, derived in the theoretical portion of this study, describe the terminal characteristics of a Hall generator. Theoretical data for curve plotting was obtained by substituting into the theoretical expressions the same magnetic field variation used in the experimental analysis. The temperatures measured for each magnetic field setting were similarly substituted into the theoretical expressions.

The results of the two analyses were curves showing the theoretical and experimental variations in input and output resistances, voltage and current gains, as functions of magnetic field and temperature. In all cases, theory and experiment were in good agreement.

5.11 Input Resistance. Input impedance curves for four different conditions were plotted. These four conditions are:

1. 50 ma input current with output open
2. 50 ma input current with output shorted
3. 500 ma input current with output open
4. 500 ma input current with output shorted

The curves for these four conditions are shown in Figs. 16 and 17, and the data listed in Table 2 of Appendix I.

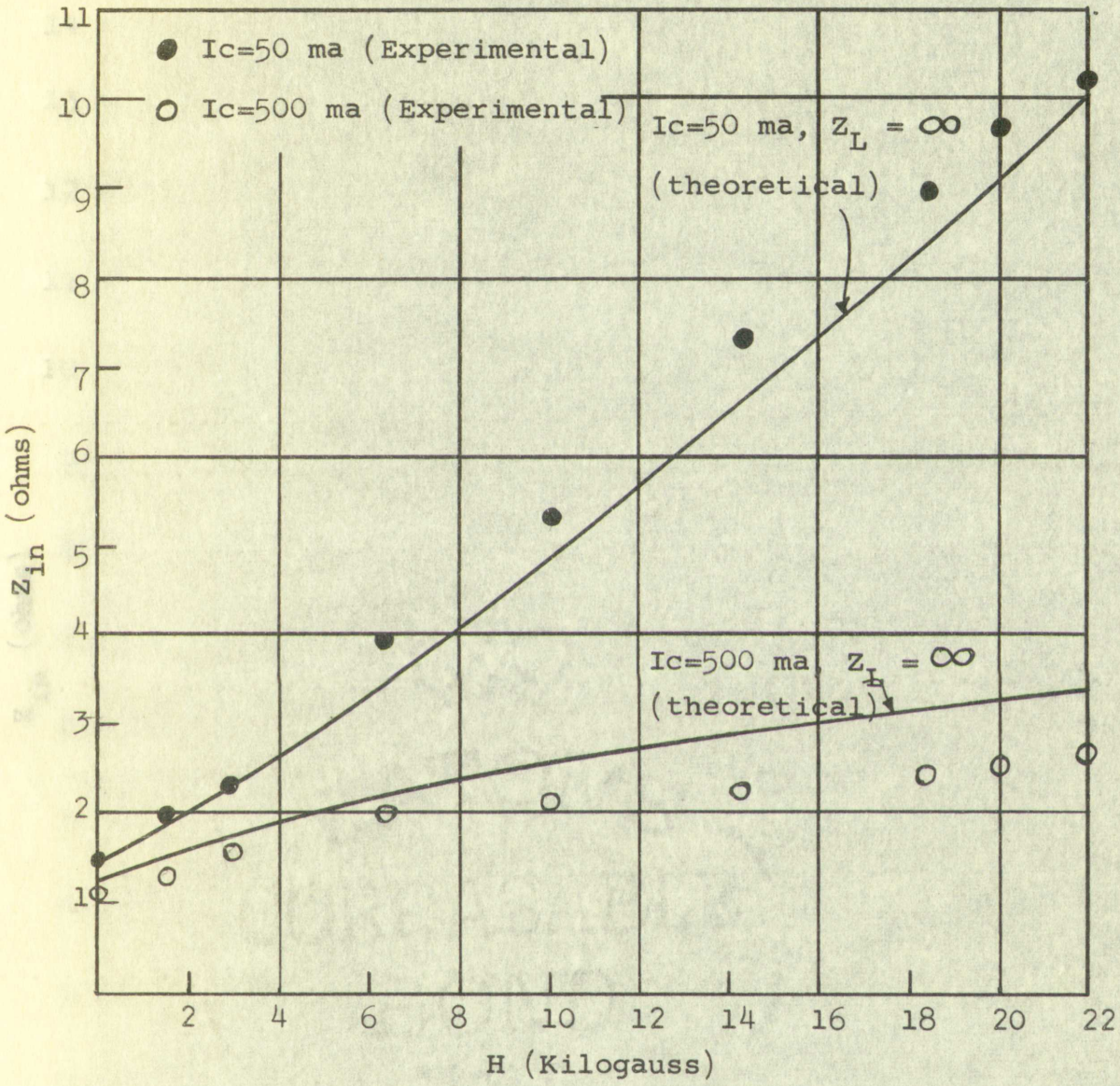

THEORETICAL AND EXPERIMENTAL CURVES
FOR INPUT RESISTANCE

FIG. 16

11
10
9
8
7
6
5
4
3
2
1
r_d' (ohms)

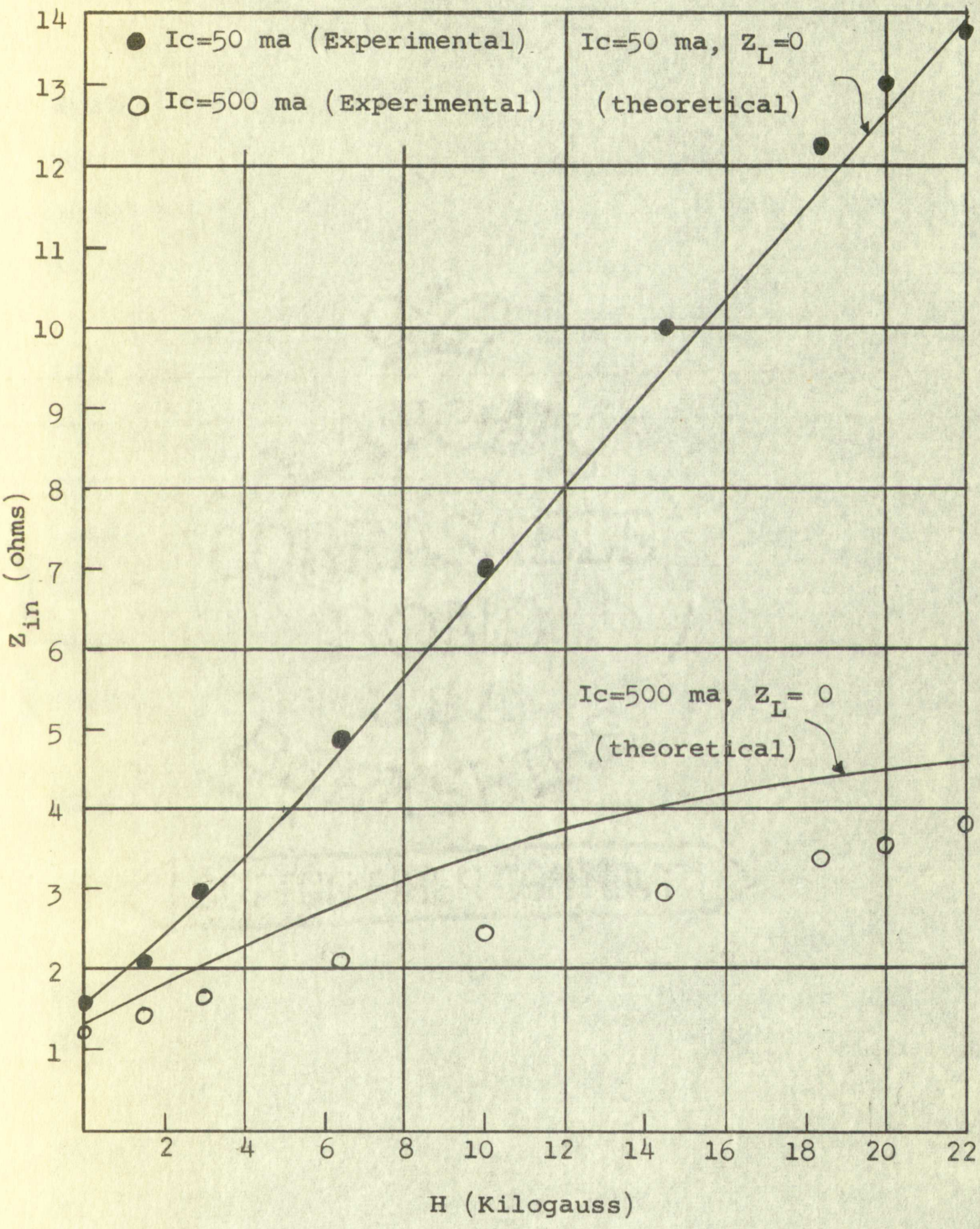

THEORETICAL AND EXPERIMENTAL CURVES
FOR INPUT RESISTANCE

FIG. 17

● Ic=50 ma (Experimental)
○ Ic=500 ma (Experimental)
S_{in} (mho)
1
2
3
4
5
6
7
8
9
10
11
12
13
14

For condition 1 the input resistance increased by seven times the original value when the magnetic field was varied from 0 to 22 kilogauss. When the output was shorted, condition 2, the resistance change was increased so that at 22 kilogauss the resistance was ten times the original value.

The 50 ma input current used in conditions 1 and 2 was low enough so that negligible heating effects occurred over the magnetic field range previously mentioned. This was not the case for 500 ma input current. An increase in sample temperature of 170° F above room temperature occurred at 22 kilogauss. This increase in temperature for increasing magnetic fields caused the conductivity to increase, thus causing the resistance change to be less pronounced.

5.12 Output Resistance. Output impedance curves were plotted for two conditions. They are:

1. 50 ma input current with an external input resistance of 140 ohms.
2. 500 ma input current with an external input resistance of 140 ohms.

Curves for these two conditions are shown in Fig. 18 and the data listed in Table 2 of Appendix I.

The change in output impedance is quite similar to the change in input impedance. For condition (1) an increase of seven times the original value occurred at 22 kilogauss, while the variation for condition 2 was less pronounced due to the heating effects.

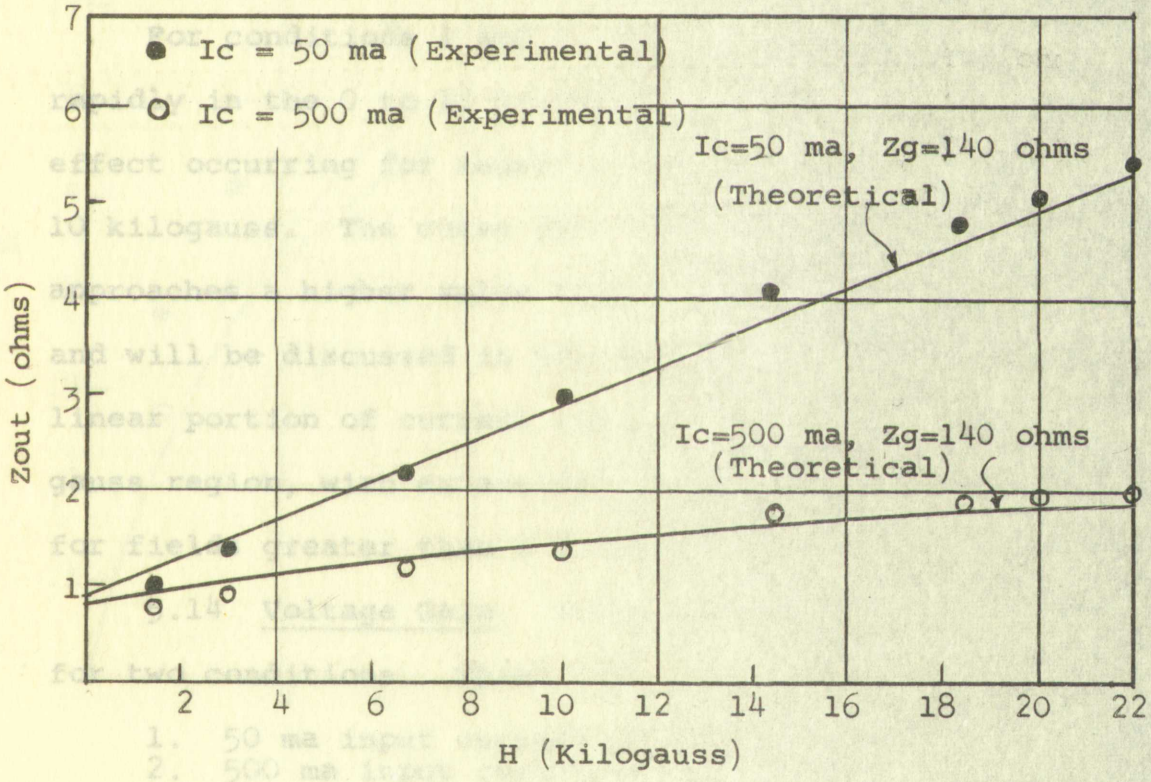

THEORETICAL AND EXPERIMENTAL
CURVES FOR OUTPUT RESISTANCE

FIG. 18

Zout (ohms)

5.13 Current Gain. Current gain curves were plotted for two conditions. These conditions are:

1. 50 ma input current with a 1/10 ohm load resistance.
2. 500 ma input current with a 1/10 ohm load resistance.

The current gain curves are shown in Fig. 19 and the data listed in Table 1 of Appendix I.

For conditions 1 and 2, the current gain increases rapidly in the 0 to 10 kilogauss region with a saturation effect occurring for magnetic field intensities greater than 10 kilogauss. The curve for condition 1 asymptotically approaches a higher value than the curve for condition 2, and will be discussed in the following section. The most linear portion of current increase lies in the 0 to 2 kilogauss region, with extensive non-linearity being encountered for fields greater than 2 kilogauss.

5.14 Voltage Gain. Voltage gain curves were plotted for two conditions. These are:

1. 50 ma input current with no load.
2. 500 ma input current with no load.

The curves are shown in Fig. 20 and data listed in Table 1 of Appendix I.

The general shape of the voltage gain curves are similar to the current gain curves. Several differences are apparent and probably the most significant is that no difference exists between curves for conditions 1 and 2, which is not

5.13 Current Gain. Current gain curves were plotted for two conditions. These conditions are:

1. 50 ma input current with a 1/10 ohm load resistance.
2. 500 ma input current with a 1/10 ohm load resistance.

The current gain curves are shown in Fig. 19 and the data listed in Table I of Appendix I.

For conditions 1 and 2, the current gain increases rapidly in the 0 to 10 kilopaus region with a saturation effect occurring for magnetic field intensities greater than 10 kilopaus. The curve for condition 1 asymptotically approaches a higher value than the curve for condition 2, and will be discussed in the following section. The most linear portion of current increase lies in the 0 to 2 kilopaus region, with extensive non-linearity being encountered for fields greater than 2 kilopaus.

5.14 Voltage Gain. Voltage gain curves were plotted for two conditions. These are:

1. 50 ma input current with no load.
2. 500 ma input current with no load.

The curves are shown in Fig. 20 and data listed in Table 4 of Appendix I.

The general shape of the voltage gain curves are similar to the current gain curves. Several differences are apparent and probably the most significant is that no difference exists between curves for conditions 1 and 2, which is not

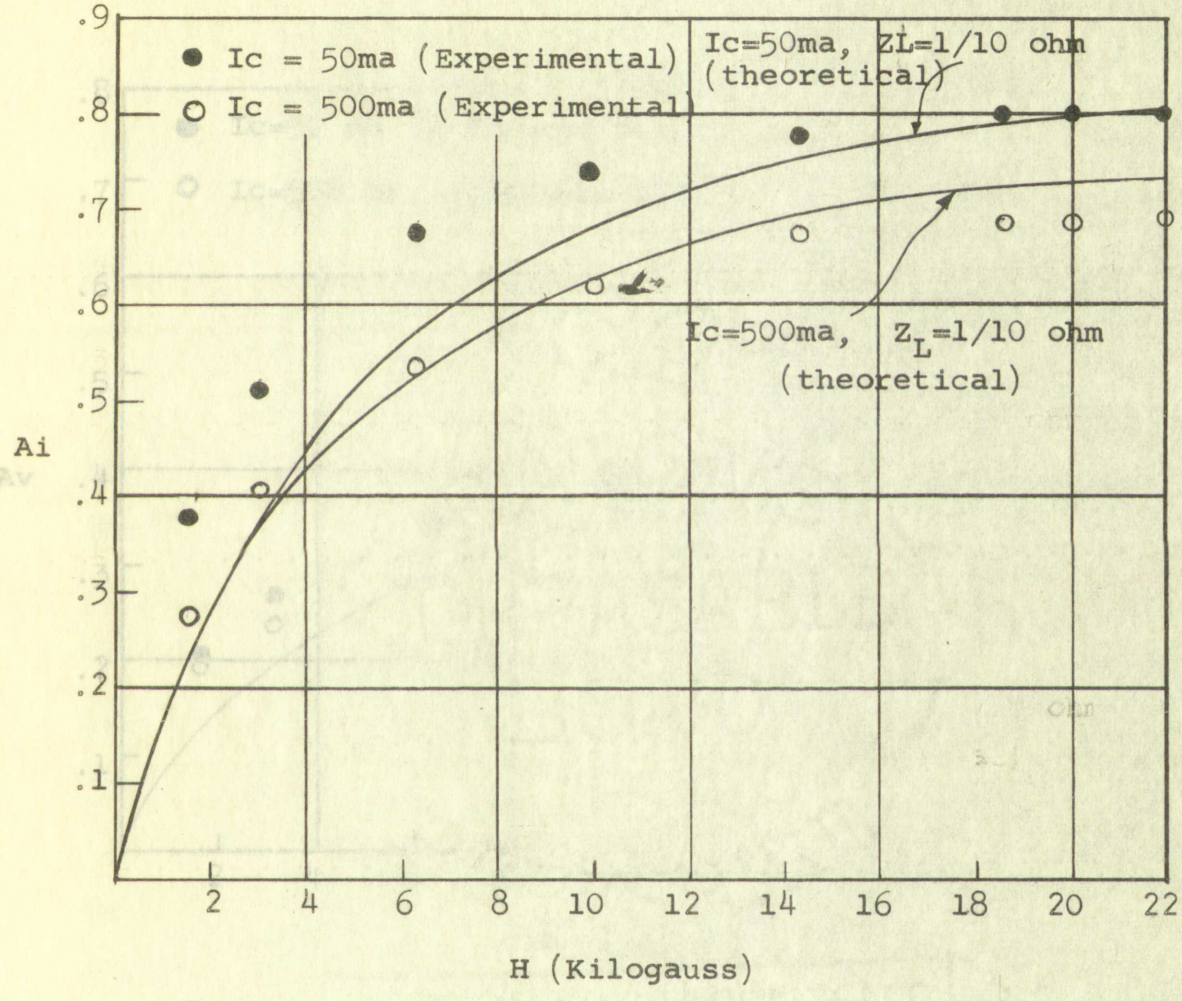

THEORETICAL AND EXPERIMENTAL CURVES
FOR CURRENT GAIN

FIG. 19

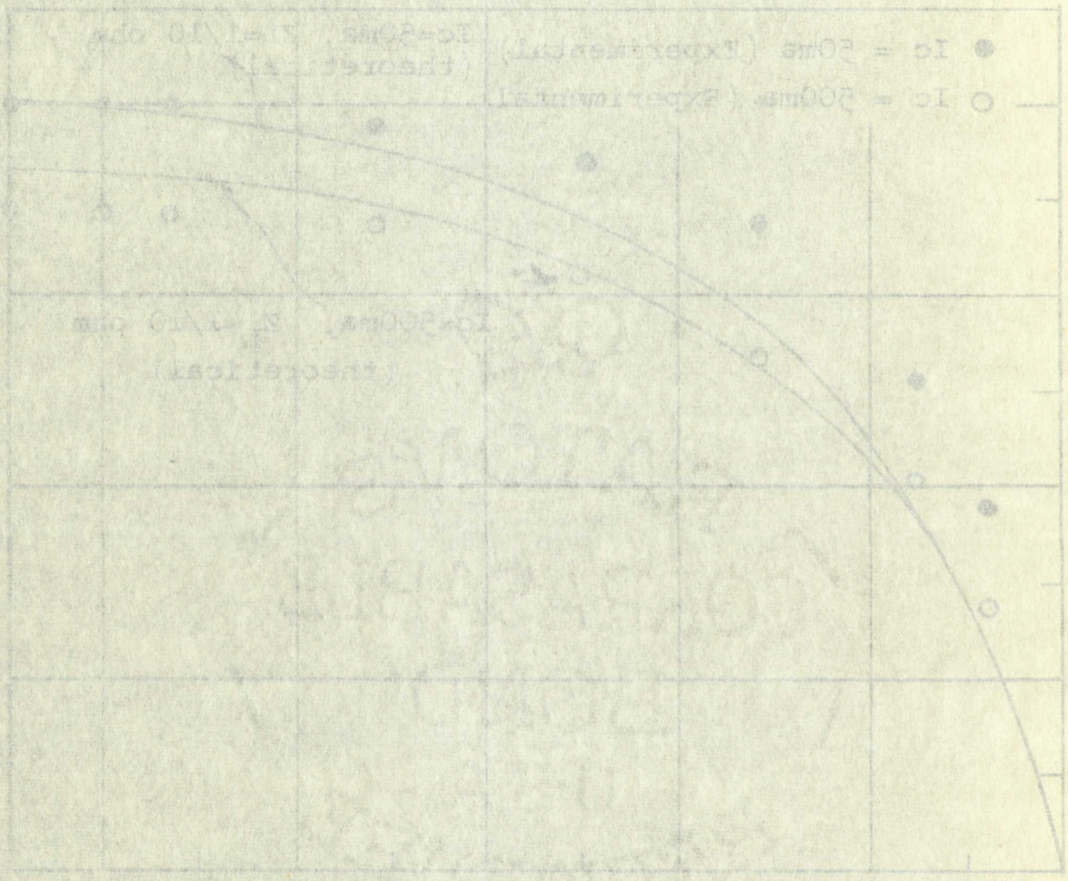

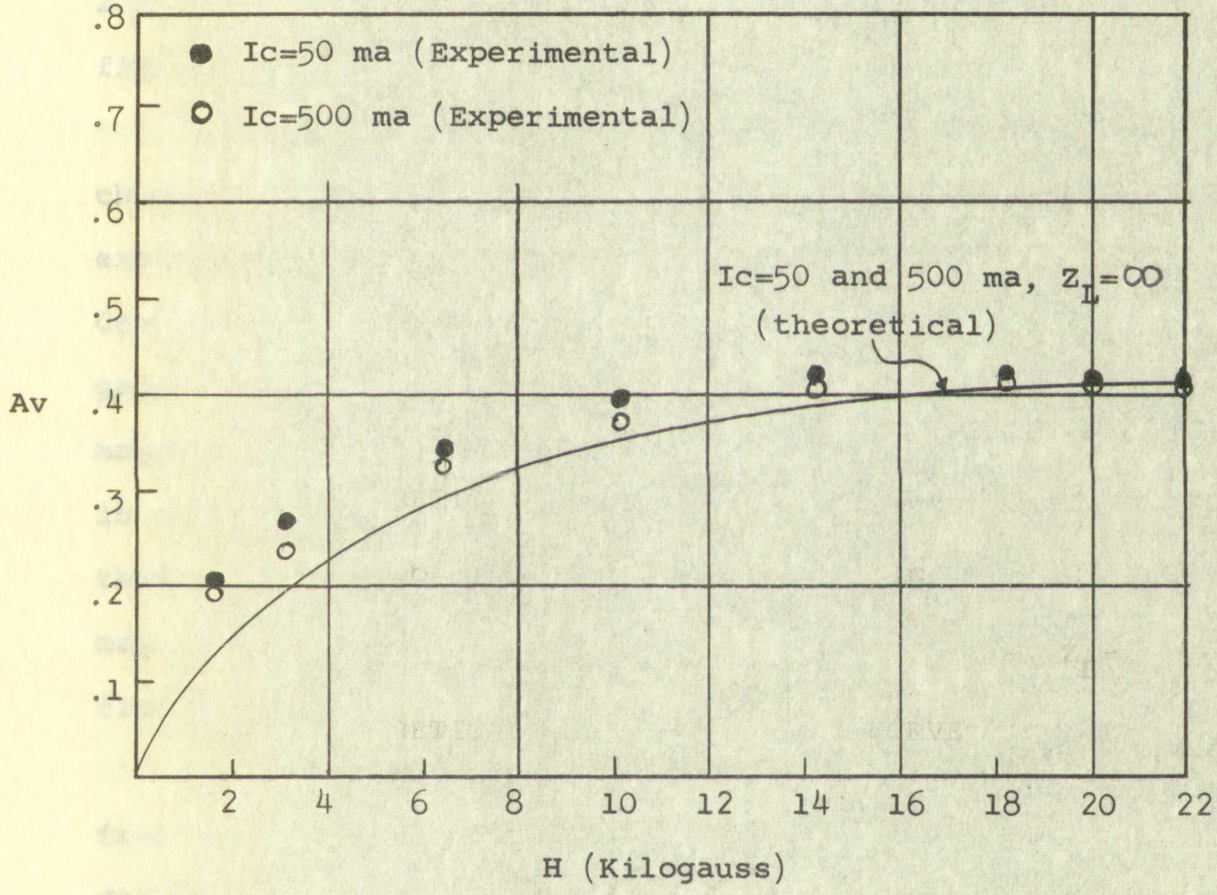

THEORETICAL AND EXPERIMENTAL CURVES
FOR VOLTAGE GAIN

FIG. 20

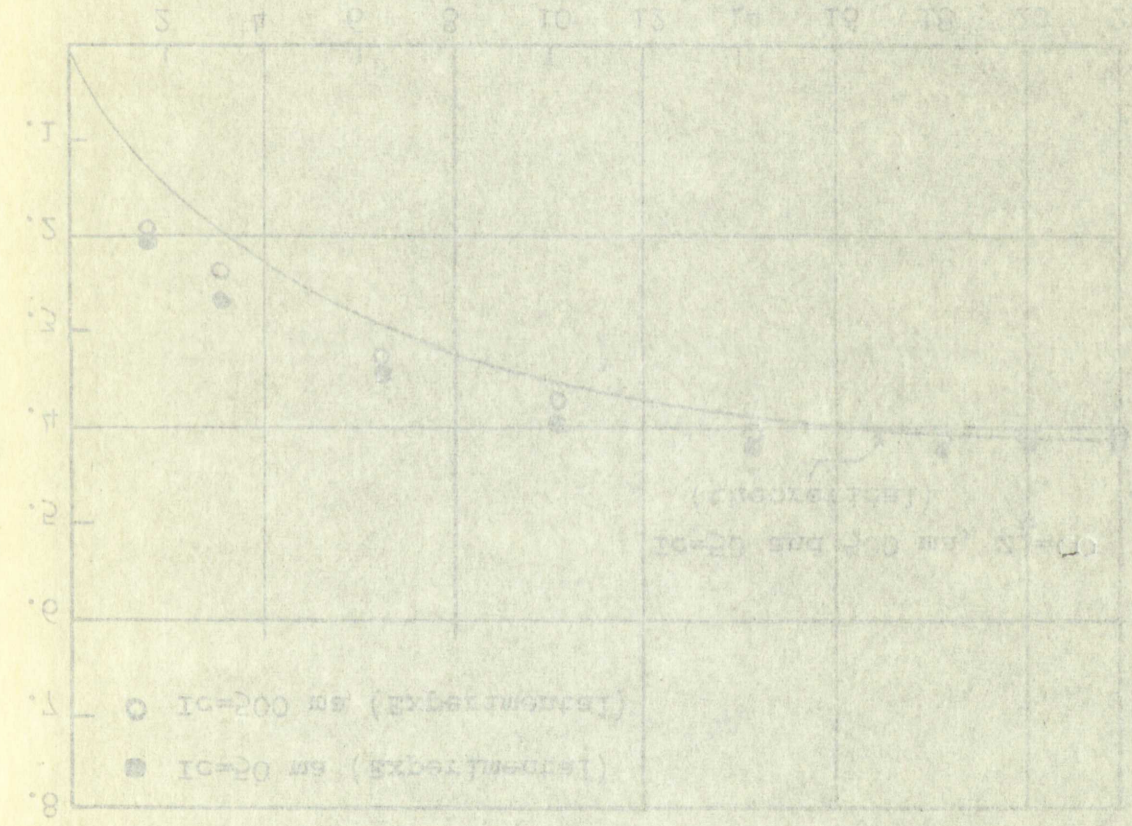

the case for current gain. This will be discussed in the following section.

A linear increase in voltage gain occurs between 0 and 2 kilogauss, while the non-linear region occurs for magnetic fields greater than 2 kilogauss.

5.2 Discussion of Curves and Data. The terminal characteristic curves, shown in the previous section, are extremely dependent upon the applied magnetic field and device temperature. In almost every case, except voltage gain, the terminal characteristics were effected by the magnitude of the input current. The final equations developed in the theoretical analysis predicted as much, but it appears that a more complete picture of the Hall generator's action may be obtained by examining the interaction of currents and fields within the device, along with the theoretical expressions.

5.21 Input Resistance. The increase in sample temperature from 50 to 500 ma input current, is sufficient to explain the difference in input resistance curves when the output is an open circuit. It is interesting to note the increase in resistance when the output is shorted (see Figs. 16 and 17). Since the temperature of the sample for a 50 ma input is unchanged when the output is shorted and open, the resistance cannot be attributed to heating effects, but rather to the change in charge distribution before and after the output is shorted.

the case for current gain. This will be discussed in the following section.

A linear increase in voltage gain occurs between 0 and 2 kilogauss, while the non-linear region occurs for magnetic fields greater than 2 kilogauss.

5.2 Discussion of Curves and Data. The terminal characteristic curves, shown in the previous section, are extremely dependent upon the applied magnetic field and device temperature. In almost every case, except voltage gain, the terminal characteristics were affected by the magnitude of the input current. The final equations developed in the theoretical analysis predicted as much, but it appears that a more complete picture of the real device action may be obtained by examining the interaction of currents and fields within the device, along with the associated experimental

5.21 Input Resistance. The increase in sample temperature from 50 to 500 ma input current, is sufficient to explain the difference in input resistance curves when the output is an open circuit. It is interesting to note the increase in resistance when the output is shorted (see figs. 10 and 17). Since the temperature of the sample rises, and hence is unchanged when the output is shorted and open, the resistance cannot be attributed to heating effects, but rather to the change in charge distribution before and after the output is shorted.

Before the output is shorted, the force created by the charge accumulation on the edges of the sample equals the force created by the cross product $v_x \times H_z$. Consequently, since there is no resultant force to deflect the carriers, the current density lines are parallel to the edges of the sample (see Fig. 21). After the output is shorted, a section of this charge is removed and the force obtained by the charge distribution no longer exists to oppose the deflecting force of the magnetic field; this allows the magnetic field to bend the current density lines in this small section of the semiconductor. When the current lines bend, they cause the carriers to follow a longer path in their excursion from electrode to electrode. At the same time the current component in the y direction combines with the magnetic field to produce a force opposing the normal drift of carriers. The combination of these effects increases the resistance of the charge depleted region (see Fig. 22) and increases the overall resistance of the sample.

5.22 Current Gain. It was previously mentioned that the only practical method to measure the output current without introducing a prohibitively large load resistance in the circuit, is to measure the voltage drop across a 1/10 ohm resistor. An examination of the current gain expression reveals that it is dependent upon the sample temperature and

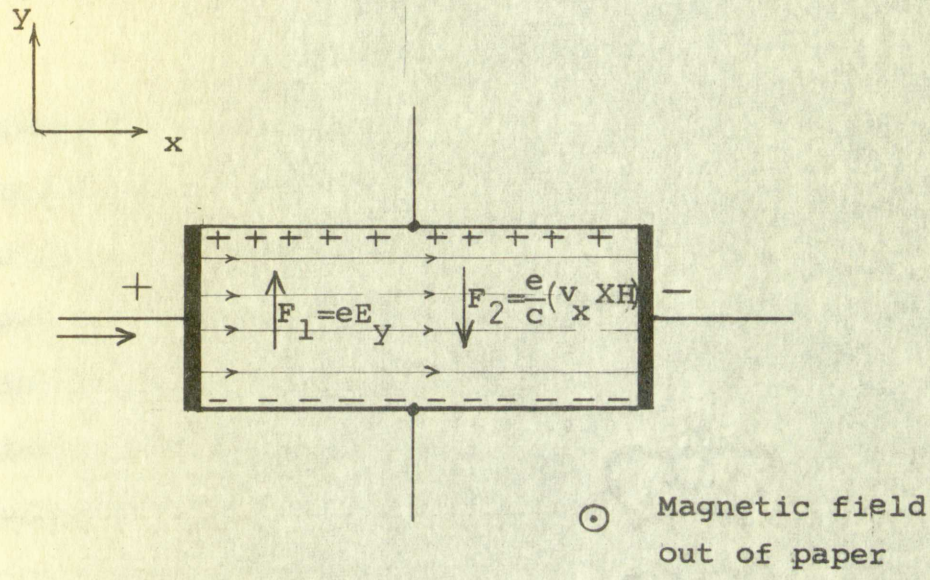

Semiconductor slab before shorted output

FIG. 21

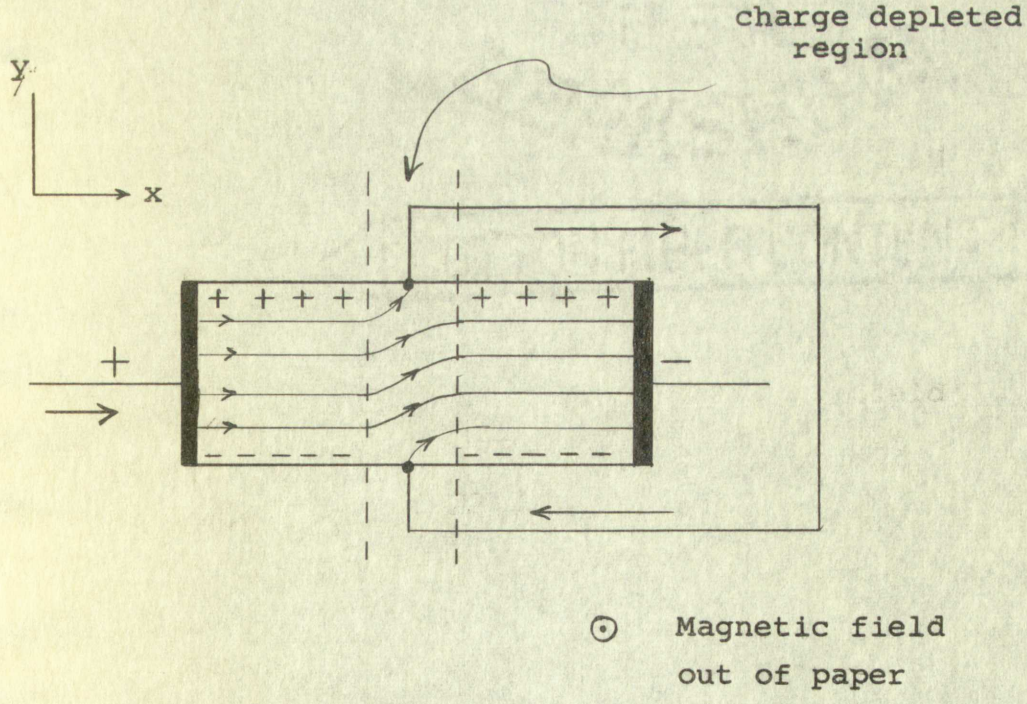

Semiconductor slab after shorted output

FIG. 22

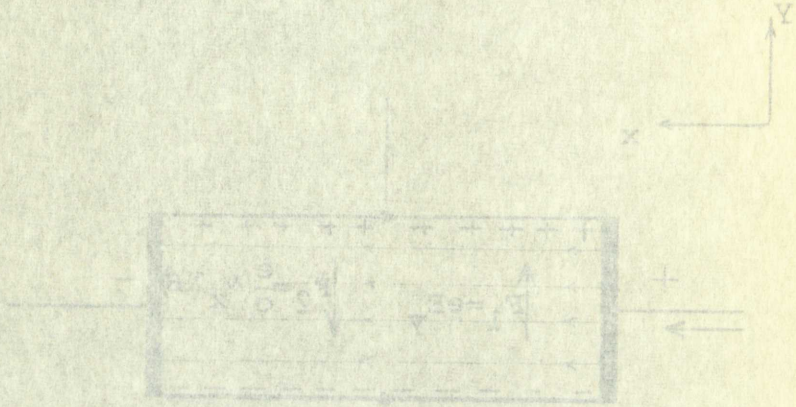
Y
X

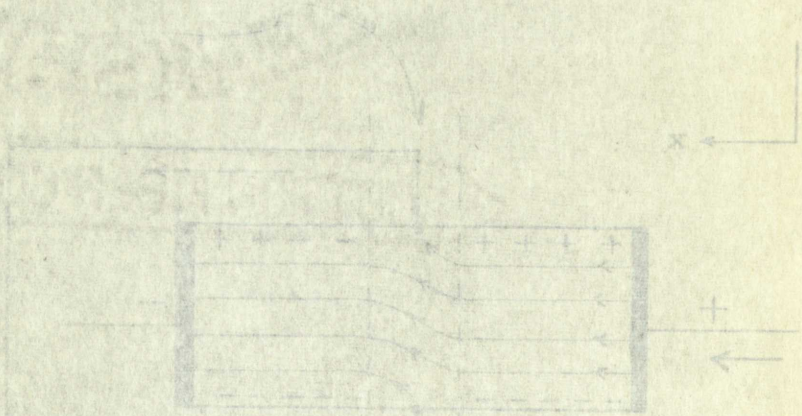
Y
X

therefore upon the input current if the output load is some value other than zero. Consequently, the higher temperatures caused the 1/10 ohm load resistor to shift both theoretical and experimental 500 ma curves to values lower than that for the 50 ma curve. Any increase in output load will decrease the output current and also magnify the effect of temperature variations.

The increase in the current gain is caused by the increasing magnetic field which diverts more carriers to the output probe. The diverted carriers circulate in the output loop, re-enter the sample at the opposite electrode, and experience a force by the electric and magnetic fields which causes them to eventually arrive at the end electrode, thus completing the input current loop (see Fig. 22).

The derived theoretical expression for current gain

$$\frac{RH\sigma l}{8_a + \sigma b Y Z_L}$$

is a function of the length/width ratio. Although the lack of different sized samples prevented experimental verification, it appears that an improvement in the current gain could be obtained by using a long thin sample.

5.23 Voltage Gain. The theoretical and experimental curves for voltage gain are independent of the device temperature. This may be explained by the fact that the experimental

data for output voltage was obtained for an infinite load. An examination of the voltage gain expression reveals that only the magnetic field variation will effect the voltage gain under these conditions. Any finite load causes a decrease in voltage gain and magnification of the temperature effect.

The voltage gain, like current gain, is a function of the length/width ratio and it appears an improvement can be made by using a very small length/width ratio. The use of a short wide sample should yield a higher voltage gain.

5.24 Output Resistance. The theoretical and experimental curves for the output resistance show a temperature and magnetic field dependence similar to the input resistance. The degree of output resistance variation will depend upon the size of the driving source impedance or the magnitude of input circuit impedance. Since the denominator of the output impedance expression has a temperature dependent term as a multiplier of the input circuit resistance, larger input circuit resistance will emphasize the effect of the temperature variations and yield a lower output resistance for increasing temperature.

CHAPTER VI

SUMMARY AND CONCLUSION

A four-terminal analysis was performed on a theoretical Hall sample to determine equations which would predict the terminal characteristics of a Hall generator. The equations were expressed as functions of sample dimensions, conductivity, Hall constant and magnetic field.

The conductivity change with temperature was determined theoretically by considering the properties of a semiconductor in the intrinsic and extrinsic conduction regions. The conductivity change with magnetic field was determined at low input currents by measuring the voltages across the sample for variations in magnetic field intensities.

The Hall constant remained reasonably constant for variations in magnetic field, but was corrected for temperature changes.

The dimensions of the experimental generator, corrections for conductivity and Hall constant were substituted into the derived equations, resulting in theoretical expressions predicting the performance of a Hall generator. The performance of a commercially produced Hall device showed the theoretical equations were in good agreement with

experimental data, for a magnetic field variation of 0 to 22 kilogauss and temperature variation of 300° to 400° Kelvin.

The experimental data was obtained from the HS-51 Halltron, a Hall generator produced by Ohio Semiconductors, Inc. The measurements for resistances, current and voltage gains are accurate to within 10%, while the temperature measurements are within 20%.

Input and output resistance variations were shown to be functions of the magnetic field, device temperature and loading. The same may be said for voltage and current gain, with the possible exception that an improvement in both could be obtained by using samples with different length/width ratios.

Since the construction of a Hall generator is quite simple, it appears that the results of the study may be applied to any Hall device of similar construction as long as the proper semiconductor dimensions, mobility, and conductivity are taken into account.

BIBLIOGRAPHY

Campbell, L. L., Galvanomagnetic and Thermomagnetic Effects, Longmans, Green and Co., New York, N. Y., 1923

Dunlap, Jr., W. C., An Introduction to Semiconductors, John Wiley, Inc., 1957

Dunlap, Jr., W. C., Physical Review, Vol. 82, 1951

Harding, J. W., Proc. Roy. Soc. London, Vol. 140A, 1933

Harman, T. C., Willardson, R. K. and Beer, A. C., Physical Review, Vol. 96, 1954

Kittel, C., Introduction to Solid State Physics, John Wiley Inc., New York, N. Y., 1956

Lindberg, O., "Hall Effect", Proc. of the IRE, Vol. 40, Nov. 1952

Panofsky, W. K. H., Classical Electricity and Magnetism, Addison-Wesley Publishing Co., Reading, Mass., 1955

Shockley, W., Electrons and Holes in Semiconductors, D. Van Nostrand Company, New York, N. Y., 1950

Sommerfeld, A. and Frank, N. H., "The Statistical Theory of Thermoelectric, Galvanomagnetic, and Thermomagnetic Phenomena in Metals", Review of Modern Physics, Vol. 3, 1931

Sommerfeld, A., Naturwissensehaften, Vol. 22, 1934

Welker, H., "Semiconducting Intermetallic Compounds", Physica, Vol. 20, 1954

Appendix I

H (Kilogauss)	Z_L = 1/10 ohm; I_C = 50 ma Theor. / Exp. A_i		Z_L = 1/10 ohm; I_C = 500 ma Theor. / Exp. A_i		Z_L = ∞; I_C = 50 & 500 ma Theor. / Exp. A_v	
	T(°K)		T(°K)		T(°K)	
0	300	0 / 0	312	0 / 0	For $Z_L = \infty$ A_v independent of T	0 / 0
1.5		.24 / .38	317	.24 / .27		.12 / .20
3.0		.39 / .51	323	.38 / .40		.20 / .24
6.5		.58 / .66	336	.51 / .52		.29 / .31
10.0		.66 / .73	351	.63 / .62		.34 / .39
14.5		.75 / .78	368	.69 / .66		.39 / .41
18.5		.79 / .80	384	.72 / .67		.40 / .41
20.0		.80 / .80	390	.73 / .67		.41 / .41
22.0		.80 / .80	398	.73 / .67		.41 / .41

Table 1

Measured Temperatures and curve data for current and voltage gains

H (Kilogauss)	$Z_L = \infty$				$Z_L = 0$				Z_g = 140 ohms			
	I_C = 50 ma Theor./Exp.		I_C = 500 ma Theor./Exp.		I_C = 50 ma Theor./Exp.		I_C = 500 ma Theor./Exp.		I_C = 50 ma Theor./Exp.		I_C = 500 ma Theor./Exp.	
	T(°K)	R_{in}	T(°K)	R_{in}	T(°K)	R_{in}	T(°K)	R_{in}	T(°K)	R_{out}	T(°K)	R_{out}
0	300	1.5/1.5	310	1.3/1.1	300	1.5/1.5	310	1.3/1.2	300	.80/.80	310	.70/.60
1.5		1.9/2.0	315	1.6/1.2		2.1/2.1	316	1.6/1.3		1.1/1.0	316	1.0/.9
3.0		2.4/2.4	321	2.0/1.5		2.9/3.0	322	2.0/1.6		1.4/1.3	323	1.1/1.1
6.5		3.5/4.0	335	2.2/2.0		4.8/4.9	334	2.8/2.1		2.1/2.1	335	1.2/1.2
10.0		4.7/5.2	346	2.5/2.1		6.8/6.9	349	3.4/2.4		3.0/3.0	350	1.3/1.3
14.5		6.8/7.1	363	2.8/2.2		9.4/10.0	366	4.0/2.9		3.8/4.1	365	1.6/1.7
18.5		8.4/8.8	375	3.1/2.4		11.8/12.2	381	4.3/3.4		4.5/4.6	380	1.7/1.8
20.0		9.0/9.5	385	3.3/2.5		12.6/13.0	387	4.4/3.6		4.9/5.0	388	1.8/1.9
22.0		10.0/10.2	390	3.4/2.6		13.9/13.8	395	4.5/3.9		5.3/5.3	395	1.9/2.0

Table 2

Measured Temperatures and curve data for input and output resistance

R (ohms)	I_C = 50 ma Theor.	Exp.	I_C = 500 ma Theor.	Exp.	I_C = 1 a Theor.	Exp.
0						
10						
20						
30						
40						
50						
60						
70						
80						
90						
100						
110						
120						
130						
140						
150						
160						
170						
180						
190						
200						
210						
220						
230						
240						
250						
260						
270						
280						
290						
300						
310						
320						
330						
340						
350						
360						
370						
380						
390						
400						
410						
420						
430						
440						
450						
460						
470						
480						
490						
500						
510						
520						
530						
540						
550						
560						
570						
580						
590						
600						
610						
620						
630						
640						
650						
660						
670						
680						
690						
700						
710						
720						
730						
740						
750						
760						
770						
780						
790						
800						
810						
820						
830						
840						
850						
860						
870						
880						
890						
900						
910						
920						
930						
940						
950						
960						
970						
980						
990						
1000						

APPENDIX II

THE SCHWARZ-CHRISTOFFEL TRANSFORMATION

Transformation of the Real Axis into a Polygon[1]

This transformation may be derived by first considering any conformal transformation $w = f(Z)$. For convenience, define unit vectors tangent to curve C in Z plane and S in W plane as

$$t = \lim_{\Delta Z \to 0} \frac{\Delta Z}{|\Delta Z|} \quad , \qquad \tau = \lim_{\Delta W \to 0} \frac{\Delta W}{|\Delta W|}$$

If the points Z and $Z + \Delta Z$ are on C, then ΔZ is a secant vector of unit length, as ΔZ and ΔW tend to zero and $f'(z) = \lim_{\Delta z \to 0} \frac{\Delta W}{\Delta Z}$ then $f'(z) = \lim_{\Delta z \to 0} \left(\frac{\Delta W / |\Delta W|}{\Delta Z / |\Delta Z|} \left| \frac{\Delta W}{\Delta Z} \right| \right) = \frac{\tau}{t} |f'(z)|$

or $\tau = \frac{f'(z)}{|f'(z)|} t$

If C is chosen to be the X axis in the traversed in the positive direction, then $t = 1$ and $\tau = \frac{f'(z)}{|f'(z)|}$.

The argument of τ is then $\arg \tau = \arg f'(Z) - \arg |f'(Z)|$

or $\arg \tau = \arg f'(Z)$, since $\arg |f'(Z)| = 0$.

If the image of the X axis is to be a polygon on n sides, the argument of $f'(Z)$ must remain constant along the X axis except for abrupt changes at n points.

---

[1] Churchill, R. V., Introduction to Complex Variables and Applications, McGraw Hill Book Co., p. 171, 1948

Transformation of the real axis

This transformation may be derived by first considering any conformal transformation $\zeta = f(z)$ which will define unit vectors tangent to curves in the Z plane and the W plane as

$$f' = \lim_{\Delta z \to 0} \frac{\Delta \zeta}{|\Delta z|}$$

If the points Z and Z + ΔZ are on C, then $\Delta\zeta$ is a unit vector of unit length as Δz and ΔW tend to zero.

$$f'(z) = \lim_{\Delta z \to 0} \frac{\Delta W}{\Delta z} \text{ then } f'(z) = \lim_{\Delta z \to 0} \left(\frac{\Delta W}{|\Delta W|} \cdot \frac{|\Delta W|}{|\Delta z|} \right)$$

or $\tau = \frac{f'(z)}{|f'(z)|}$

If C is chosen to be the X axis in the direction of the positive direction, then $\zeta = \xi$ and $\tau = \frac{f'(z)}{|f'(z)|}$

The argument of τ is then $\arg \tau = \arg f'(z) - \arg f'(z)$ or $\arg \tau = \arg f'(z)$.

If the image of the X axis is to be a polygon on a circle the argument of $f'(z)$ must remain constant except for abrupt changes at a point

---

[1] Churchill, R. V., Introduction to Complex Variables and Applications, McGraw Hill Book Co., p. 1, 1948.

The values of Z along the real axis for which arg f'(Z) changes as a point Z moves along the axis are X_1, X_2, ... , X_{n-1} and $Z = \infty$

X_1, X_2, etc. are chosen such that $X_1 < X_2 < .... < X_{n-1}$. If W_n denotes the value of f(Z) as Z tends to infinity and if $W_j = f(Z_j)$ for j = 1,2,3...., n-1, the points W_1, W_2, ... , W_n will be the vertices of the polygon. If a function f(Z) is chosen such that

$$f'(Z) = A(Z-X_1)^{-k_1}(Z-X_2)^{-k_2} \ldots (Z-X_{n-1})^{-K_{n-1}}$$

where A is a complex constant and K_g is a real constant, then its argument can be written as

$$\arg f'(Z) = \arg A - K_1 \arg(Z-X_1) - K_2 \arg(Z-X_2) - \ldots - K_{n-1}\arg(Z-X_{n-1}).$$

When Z = X and $X < X_1$,

$$\arg(Z-X_1) = \arg(Z-X_2) = \ldots = \arg(Z-X_{n-1}) = \pi$$

When $X_1 < X < X_2$ the argument of $(Z-X_1)$ is zero while the others are π. According to the equation arg f'(Z) increases by angle $K_1\pi$ as Z moves through X_1 from the left. It again increases, by the angle $K_2\pi$, as Z passes through X_2, etc.

Since $\arg\tau = \arg f'(Z)$, then τ is constant as Z moves along any segment of the X axis between two points or the path of W is a straight line. The direction of τ abruptly changes at W_j corresponding to $Z = Z_j$ in fact, arg τ increases by $K_j\pi$ at those points. (Fig. 1)

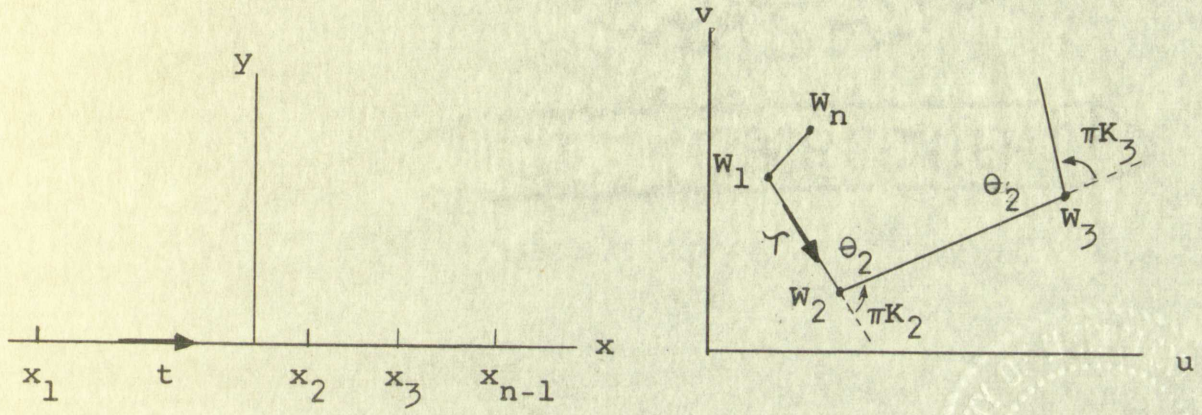

Fig. 1

Under this transformation $W = f(Z)$, the image of the X axis is therefore a polygon with exterior angles $K_j\pi$ at vertices W_j.

The sum of the exterior angles of any closed polygon is 2π. The exterior angle at W_n which is the image of Z = is given by

$$K_n\pi = 2\pi - (K_1 + K_2 + \ldots + K_{n-1})\pi$$

If $K_1 + K_2 + \ldots + K_{n-1} = 2$, then $K_n = 0$ and the last side and first side have the same direction; thus W_n is not a vertice but a point on the first side.

If K_j is written in terms of the interior angle θ_j then $K_j\pi + \theta_j = \pi$ or $K_j = 1 - \frac{1}{\pi}\theta_j$. The transformation can be written as

$$\frac{dW}{dz} = A(z-x_1)^{\left(\frac{\theta_1}{\pi}-1\right)}(z-x_2)^{\left(\frac{\theta_2}{\pi}-1\right)}\ldots(z-x_n)^{\left(\frac{\theta_n}{\pi}-1\right)}$$

or

$$\frac{dW}{dz} = A\prod_{\lambda=1}^{n}(z-x_\lambda)^{\left(\frac{\theta_\lambda}{\pi}-1\right)}$$